



Calhoun: The NPS Institutional Archive

Theses and Dissertations

Thesis Collection

1951

Emissivity calculation for carbon monoxide.

Ostrander, Max H.

California Institute of Technology

<http://hdl.handle.net/10945/14142>



Calhoun is a project of the Dudley Knox Library at NPS, furthering the precepts and goals of open government and government transparency. All information contained herein has been approved for release by the NPS Public Affairs Officer.

Dudley Knox Library / Naval Postgraduate School
411 Dyer Road / 1 University Circle
Monterey, California USA 93943

<http://www.nps.edu/library>

GUGGENHEIM AERONAUTICAL LABORATORY
CALIFORNIA INSTITUTE OF TECHNOLOGY

EMISSIVITY CALCULATIONS FOR CARBON MONOXIDE

By

Max H. Ostrander

LCDR, USN

PASADENA, CALIFORNIA

THESES
086





EMISSIVITY CALCULATIONS FOR CARBON MONOXIDE

Thesis by
M. H. Ostrander
Lieutenant Commander, U. S. Navy

In Partial Fulfillment of the Requirements
for the Degree of
Aeronautical Engineer

California Institute of Technology
Pasadena, California

1951

ACKNOWLEDGMENT

It is with sincere appreciation that the author acknowledges the ever-ready assistance of Dr. S. S. Penner of the California Institute of Technology in extending the instruction, references, and helpful criticism that were of such assistance in the preparation of this report.

ABSTRACT

The purpose of this report is to utilize a sound theoretical formulation, combined with the best available experimental data on integrated absorption and rotational line-width, for the calculation of emissivities of carbon monoxide at room temperatures under conditions where overlapping between rotational lines is negligibly small.

The results of the present investigation indicate that calculated emissivities of carbon monoxide at room temperature are in excellent agreement with empirically observed data published by Hottel and Ullrich. The theoretical dependence of emissivity upon optical density at low optical density and at room temperature has been shown to follow the experimental observations almost exactly. For low optical densities the calculated emissivity is found to be nearly proportional to the assumed rotational line-width, thus emphasizing the need for accurate line-width determinations at all temperatures. The calculated dependence of emissivity on rotational line-width permits the determination of emissivity not only as a function of temperature, total pressure, and optical density, but also as a function of concentration of optically inert gas. For numerical calculations of this type it is necessary to obtain experimental data for the dependence of rotational line-width on the concentration of non-emitting gases.

The present calculations supplement earlier theoretical emissivity calculations, which are valid only at elevated total pressures where extensive overlapping of rotational lines occurs. The range of pressures in which overlapping between rotational lines is neither extensive nor negligibly small has been considered only very briefly and requires further examination.

TABLE OF CONTENTS

PAGE		PAGE
ACKNOWLEDGMENT		ii
ABSTRACT		iii
LIST OF TABLES		vi
LIST OF FIGURES		viii
TABLE OF SYMBOLS		ix
I.	INTRODUCTION	1
II.	FUNDAMENTAL THEORETICAL RELATIONS OF RADIANT HEAT TRANSFER	5
III.	BASIC NUMERICAL DATA	12
	A. Determination of Line Widths	12
	B. Calculation of Line Centers Vibrational- Rotation Transitions	13
	C. Numerical Calculation of Integrated Absorption of Rotational Lines	27
	D. Methods for the Determination of the Complete Partition Function	35
IV.	EMISSIVITY CALCULATIONS FOR DIATOMIC GASES WITH NON-OVERLAPPING ROTATIONAL LINES	38
V.	NUMERICAL EMISSIVITY CALCULATIONS FOR CARBON MONOXIDE AT 300°K	43
	A. Overlapping Between Adjacent Rotational Lines	43

<u>PART</u>		<u>PAGE</u>
B.	Description of Emissivity Calculations for CO Assuming No Overlapping Between Rotational Lines	45
C.	Effect of Rotational Half-Width on Emissivity	58
D.	Emission of Radiation from the First Overtone of CO at 300°K and Atmospheric Pressure	61
VI.	CONCLUSIONS AND RECOMMENDATIONS FOR FURTHER STUDY	62
REFERENCES		64
FIGURES		66

LIST OF TABLES

<u>NUMBER</u>	<u>PAGE</u>
I. WAVE NUMBERS (cm^{-1}) CORRESPONDING TO ENERGY TRANSITIONS FOR THE FUNDAMENTAL VIBRATION-ROTATION BAND OF CO $n \rightarrow n + 1, j = -1$	15
II. WAVE NUMBERS (cm^{-1}) CORRESPONDING TO ENERGY TRANSITIONS FOR THE FUNDAMENTAL VIBRATION-ROTATION BAND OF CO $n \rightarrow n + 1, j = +1$	17
III. WAVE NUMBERS (cm^{-1}) CORRESPONDING TO ENERGY TRANSITIONS FOR THE VIBRATION-ROTATION BAND OF THE FIRST OVERTONE OF CO $n \rightarrow n + 2, j = -1$	19
IV. WAVE NUMBERS (cm^{-1}) CORRESPONDING TO ENERGY TRANSITIONS FOR THE VIBRATION-ROTATION BAND OF THE FIRST OVERTONE OF CO $n \rightarrow n + 2, j = +1$	21
V. WAVE NUMBERS (cm^{-1}) CORRESPONDING TO ENERGY TRANSITIONS FOR THE VIBRATION-ROTATION BAND OF THE SECOND OVERTONE OF CO $n \rightarrow n + 3, j = -1$	23
VI. WAVE NUMBERS (cm^{-1}) CORRESPONDING TO ENERGY TRANSITIONS FOR THE VIBRATION-ROTATION BAND OF THE SECOND OVERTONE OF CO $n \rightarrow n + 3, j = +1$	25

NUMBER	PAGE
VII. TABULATED INTEGRATED ABSORPTIONS FOR CARBON MONOXIDE AT 300°K (FUNDAMENTAL VIBRATION-ROTATION BAND)	31
VIII. TABULATED INTEGRATED ABSORPTIONS FOR CARBON MONOXIDE AT 500°K (FUNDAMENTAL VIBRATION-ROTATION BAND)	32
IX. TABULATED INTEGRATED ABSORPTIONS FOR CARBON MONOXIDE AT 1000°K (FUNDAMENTAL VIBRATION-ROTATION BAND)	33
X. TABULATED INTEGRATED ABSORPTIONS FOR CARBON MONOXIDE AT 300°K (FIRST OVERTONE)	34
XI. Q_{vjm} FOR CO (ASSUMED AN IDEAL DIATOMIC GAS) AS A FUNCTION OF TEMPERATURE	36
XII. Q_{vjm} FOR CO (GENERAL DIATOMIC GAS, VIBRATION-ROTATION INTERACTION) AS A FUNCTION OF TEMPERATURE	37
XIII. CALCULATION OF THE TERM X_j FOR TWO GIVEN TRANSITIONS	47
XIV. CALCULATION OF THE TERM $F(X_j)$ FOR TWO GIVEN FUNCTIONS	48
XV. INTERMEDIATE STEPS FOR THE CALCULATION OF RADIANT INTENSITY FOR TWO GIVEN TRANSITIONS	50
XVI. (a&b) WORK SHEET FOR THE CALCULATION OF THE EMISSIVITY OF CARBON MONOXIDE AT 300°K. ($\alpha = 0.08 \text{ cm}^{-1}$, $pL = 0.1$) ($j \rightarrow j \pm 1$)	51-54
XVII. (a&b) WORK SHEET FOR THE CALCULATION OF R_λ / ν^2 FOR THE FUNDAMENTAL VIBRATION-ROTATION BAND OF CO AT 300°K ($j \rightarrow j \pm 1$)	55-56
XVIII. EMISSIVITIES AT 300°K AND ATMOSPHERIC PRESSURE FOR NON- OVERLAPPING ROTATIONAL LINES ($\alpha = 0.08 \text{ cm}^{-1}$)	57
XIX. TABULATED RESULTS OF CALCULATED AND OBSERVED EMISSIVITIES	59-60

LIST OF FIGURES

<u>NUMBER</u>		<u>PAGE</u>
1	SPECTRAL ABSORPTION COEFFICIENT ρ_ν AS A FUNCTION OF AT 300°K FOR $\alpha = 0.06 \text{ cm}^{-1}$	66
2	SPECTRAL EMISSIVITY AS A FUNCTION OF WAVE NUMBER FOR VARIOUS OPTICAL DENSITIES FOR TWO ADJACENT INTENSE ROTATIONAL LINES ($j = 8 \rightarrow j = 7$ and $j = 7 \rightarrow j = 6$)	67
3	SPECTRAL EMISSIVITY AS A FUNCTION OF WAVE NUMBER FOR VARIOUS OPTICAL DENSITIES FOR TWO ADJACENT WEAK ROTATIONAL LINES ($j = 19 \rightarrow j = 18$ and $j = 18 \rightarrow j = 17$)	68
4	VARIATION OF CALCULATED EMISSIVITY WITH SPECTRAL HALF- WIDTH	69

TABLE OF SYMBOLS

A	intensity of light absorbed in a wave number interval (ν to $\nu + d\nu$)
c	velocity of light
c_1	$2\pi c^2 h = 3.740 \times 10^{-5} \text{ erg} \cdot \text{cm}^{-2} \cdot \text{sec}^{-1}$
c_2	$ch/k = 1.436 \text{ cm} \cdot {}^\circ\text{K}$
E	energy
h	Planck's constant
i	upper energy level
I_j	intensity of radiant energy emitted by a particular vibration-rotation transition
I_ν	intensity of radiant energy emitted in a wave number interval (ν to $\nu + d\nu$)
I_ν'	intensity of radiant energy emitted in frequency interval (ν' to $\nu' + d\nu'$)
I_ν^0	intensity of radiant energy emitted by a blackbody in a wave number interval (ν to $\nu + d\nu$)
$I_{0\nu}$	intensity of incident radiant energy in a wave number interval (ν to $\nu + d\nu$)
j	lower energy level; rotational quantum number
J_ν	intensity of radiation in a wave number interval (ν to $\nu + d\nu$)
J_ν^0	intensity of radiation by a blackbody in a wave number interval (ν to $\nu + d\nu$)
k	Boltzmann's constant
L	optical path length
n	vibrational quantum number

p	pressure
p _L	optical density
F _v	spectral absorption coefficient
R _λ	energy emitted by a blackbody in a wave length interval (λ to $\lambda + d\lambda$)
R _{λmax}	maximum value of R _λ
R _{0+∞}	energy emitted by a blackbody over all wave lengths
S	integrated absorption
T	absolute temperature

GREEK SYMBOLS

α	spectral half-width
α _c	collision half-width
α _D	Doppler half-width
E	effective charge, emissivity
E _r	spectral emissivity
λ	wave length
μ	reduced mass
ν	wave number
ν _i	frequency
ρ(v)	density of radiation
σ	Stephan-Boltzmann constant

I. INTRODUCTION

The study of radiant heat transfer and related problems has been given great impetus in the past decade by the development of propulsive systems which demand that engine and motor components withstand increasingly higher temperatures. Improvement of the engine and motor components requires, among other things, knowledge of radiant heat transfer, which can be expressed as a function of the emissivities of the gases formed by combustion. Although considerable experimental research has been done on the measurement of gas emissivities, it has become increasingly evident that physical limitations prohibit the direct experimental determination of gaseous emissivities at the temperatures and pressures which are encountered in combustion chambers. For this reason it is of obvious practical importance to develop theoretical methods for making emissivity calculations.

The general problem of emission and absorption of radiation involves two essentially distinct types of analysis. One important branch of radiant heat transfer investigations is concerned with the determination of radiant intensities if emissivities, absorptivities, and scattering coefficients are known. These studies deal with the problem of radiative transfer only. For any defined geometric arrangement, the radiative transfer problems can be formulated without difficulty. An exhaustive account of this work may be found in a recently published book by Chandrasekhar⁽¹⁾.

Since radiant heat transfer calculations require detailed knowledge of emissivities, absorptivities, and scattering coefficients, it is essential to consider methods for the determination of these quantities.

The quantum-mechanical problems involved in the theoretical calculation of emissivity were solved, in principle, some years ago. The results of those theoretical studies have been applied, to a limited extent, in the use of spectroscopic measurements for flame temperature determination from line intensities⁽²⁾, and for the analysis of absorption and emission of radiation in the atmosphere⁽³⁾. An important paper by Dennison⁽⁴⁾, written more than twenty years ago, contains some of the basic theoretical relations which have been used for numerical emissivity calculations on carbon monoxide in the present studies.

Earlier emissivity calculations^(3,5,6) for diatomic molecules at elevated total pressures were based upon the assumption that the overlapping of the rotational lines was so extensive that the spectral absorption coefficient was not a rapidly varying function of the wave number. With this assumption, approximate emissivity calculations were carried out using an average spectral absorption coefficient over an effective width^(5,6,7) corresponding to an entire vibration-rotation band. Reliable emissivity measurements at elevated total pressures are not yet available for an empirical verification of these calculations. Therefore, the calculations were compared with measurements made by Ullrich and Hottel at atmospheric pressure. At atmospheric pressure, the assumption of extensive overlapping of the rotational lines does not apply and it was not unexpected to find that experimentally determined emissivities at low optical densities were considerably lower than the calculated values. The observed discrepancies are the result of the fact that the broadening of the rotational lines at atmospheric pressure is far less than is necessary to justify the use of average absorption

coefficients. For increasing values of optical density, the experimental emissivity measurements were found to approach and then exceed the calculated emissivities as the weaker rotational lines, which lie outside the range of the estimated bandwidth, contributed more and more to the radiant heat transfer. These results indicate that this approximate method of radiant heat transfer calculations is valid for the conditions for which it was developed, i.e., extensive overlapping of rotational lines at elevated total pressures such that an average spectral absorption coefficient could be used over an effective width corresponding to the entire band.

It is of obvious importance to apply a method for the calculation of emissivities under conditions for which overlapping of rotational lines is negligibly small. Such a method is available as the result of extension of a theoretical treatment developed by Elsasser⁽³⁾, whose work applied only to equally intense and equally spaced rotational lines which did not overlap. The extension to this treatment⁽³⁾ applies to any system with non-overlapping lines.

The extent of overlapping of rotational lines is a function not only of total pressure but also of optical density. In this report, numerical emissivity calculations have been carried out for carbon monoxide to supply values of emissivity which are reliable only at small optical densities, i.e., under conditions such that overlapping of rotational lines may be neglected. Under these conditions the line shape may be represented by a dispersion formula. Use of the best available experimental data on integrated absorption and rotational line-width leads to calculated emissivities at room temperatures which

are in excellent agreement with empirically observed data published by Ullrich and Hottel⁽⁹⁾. The theoretical dependence of emissivity upon optical density at room temperature has been shown to follow the experimental observations almost exactly.

For low optical densities, the calculated emissivity is found to be nearly proportional to the assumed rotational line-width, thus emphasizing the need for accurate line-width determinations at elevated temperatures. The calculated dependence of emissivity on rotational line-width permits the determination of emissivity not only as a function of temperature, total pressure, and optical density, but also as a function of concentration of optically inert gas. For numerical calculations of this type it is necessary to have experimental data for the dependence of rotational line-width on the concentration of non-emitting gases.

III. FUNDAMENTAL THEORETICAL RELATIONS OF RADIANT HEAT TRANSFER

As a background for the numerical calculations which follow, this section will be devoted to a presentation of the basic theoretical equations of radiant heat transfer.

Radiation from a heated gas originates with a transition from an excited energy level to a lower energy level. These transitions may correspond to changes in electronic, vibrational, or rotational energy. The electronic transitions, involving much greater energy changes than the others, generally produce radiation in either the visible or ultraviolet regions of the spectrum. Vibration-rotation transitions lead to emission in the near infrared and infrared regions of the spectrum.

A radiating gas emits energy over a well-defined range of frequencies, each individual transition contributing to this range. The total radiation is obtained by summing the radiant intensities corresponding to the individual transitions. A theoretical calculation requires the knowledge of:

(a) The number of molecules and atoms in each of the various energy levels. With the assumption of thermal equilibrium, this distribution can be calculated from quantum statistics.⁽¹⁰⁾

(b) The frequencies corresponding to these transitions must be known. Spectroscopic measurements are available which will permit these frequencies to be calculated with a high degree of accuracy.^(11,12)

(c) The spectral line shape must be known as a function of temperature and pressure. Although this information is not known accurately, calculations of Doppler half-width and the effect of collision broadening based on recently published infrared absorption measurements⁽¹³⁾ may

permit satisfactory estimates.

(d) For given transitions, the intensities of radiation depend on the transition probabilities which are related to the experimentally determined value of the integrated absorption. (4,14,15,16)

At ordinary temperatures the only important contributions to radiant heat transfer originate with the infrared vibration-rotation bands. Therefore, calculations will be restricted to this spectral region. At room temperature the problem may be simplified further since only collision broadening makes important contributions to the linewidth.

The spectral radiation intensity emitted by a blackbody is given by the well-known Planck distribution law:

$$\rho(\nu') d\nu' = \frac{8\pi h \nu'^3}{c^3} [e^{\frac{h\nu'}{kT}} - 1]^{-1} d\nu' \quad (1)$$

Here $\rho(\nu') d\nu'$ represents the density of radiation in unit volume in the frequency range between ν' and $\nu' + d\nu'$, h represents Planck's constant, c is the velocity of light, k equals the Boltzmann constant, and T is the absolute temperature of the blackbody emitter. It follows that $I_{\nu'} d\nu' = c\rho(\nu') d\nu'$ represents the radiant energy emitted per unit area of blackbody per unit time in the frequency interval between ν' and $\nu' + d\nu'$.

According to the basic law for the absorption of monochromatic radiation, the fractional decrease in spectral light intensity is proportional to the optical density, i.e.,

$$-\left(\frac{1}{I_\nu}\right)\left(\frac{d I_\nu}{d(\rho L)}\right) = P_\nu \quad (2)$$

where pL represents the optical density (i.e., the product of the optical path length L and the partial pressure of the gaseous absorber p), and ρ_ν is the spectral absorption coefficient.

Integration of Eq. (2) results in the expression:

$$I_\nu = I_{0\nu} e^{-\rho_\nu pL} \quad (3)$$

where I_ν is the intensity of transmitted light in the spectral region between ν and $\nu + d\nu$, and $I_{0\nu}$ is the intensity of the incident light in the same spectral range. The intensity of the light absorbed is, therefore,

$$A_\nu = I_{0\nu} - I_\nu = I_{0\nu} (1 - e^{-\rho_\nu pL}) \quad (4)$$

According to Kirchhoff's law the ratio of the spectral emissivity to the spectral absorptivity is unity for all substances which are in thermal equilibrium. The emissivity is defined as the ratio of the intensity of radiation emitted by a substance per unit area of emitter per unit time under specified conditions of temperature and pressure, divided by the intensity of radiation emitted by a blackbody per unit area per unit time under the same conditions. The absorptivity (i.e., the fraction of radiation absorbed) is evidently $1 - e^{-\rho_\nu pL}$ by Eq. (4). Hence it follows from Kirchhoff's law that the emissivity is also given by the expression

$$\epsilon_\nu(\tau) = 1 - e^{-\rho_\nu pL} \quad (5)$$

where both the spectral emissivity (ϵ_ν) and the spectral absorption coefficient (ρ_ν) are functions of the wave number ν and the absolute

temperature T.

The dispersion formula of Lorentz, which is known to give a satisfactory representation of line shape at moderate pressures and at temperatures low enough to permit neglect of Doppler broadening, may be written as

$$P_\nu = \frac{\alpha_{ij} S_{ij}}{(\nu - \nu_{ij})^2 + \alpha_{ij}^2} \quad (6)$$

for a single rotational line. The term S_{ij} represents the integrated absorption for the line whose center lies at the wave number ν_{ij} . The quantity α_{ij} is the spectral half-width, which is defined as that frequency interval for which the absorption is greater than one-half of its maximum value. The wave numbers represented by ν_{ij} may be calculated from the Bohr frequency rule.

The spectral absorption coefficient P_ν resulting from all the rotational transitions of the fundamental vibration-rotation band is, by an obvious extension of Eq. (6),

$$P_\nu = \frac{\alpha}{\pi} \sum_j \left[\frac{S_{j \rightarrow j+1}^{0 \rightarrow 1}}{(\nu - \nu_{j \rightarrow j+1}^{0 \rightarrow 1})^2 + \alpha^2} + \frac{S_{j+1 \rightarrow j}^{0 \rightarrow 1}}{(\nu - \nu_{j+1 \rightarrow j}^{0 \rightarrow 1})^2 + \alpha^2} \right] \quad (7)$$

where

$S_{j \rightarrow j \pm 1}^{0 \rightarrow 1}$ = the integrated absorption for the transition in which the vibrational quantum number changes from 0 to 1 and the rotational quantum number from j to $j \pm 1$,

α = the rotational half-width of the spectral lines
 which is assumed to be the same for all of
 the rotational lines,

$\nu_{j \rightarrow j \pm 1}^{0 \rightarrow 1}$ = the wave number of the line center of the
 indicated transition.

At elevated temperatures the value of P_ν in the region of the fundamental vibration-rotation band will be influenced by the contribution from transitions involving energy states above the first excited vibrational level. This influence can be accounted for by including an appropriate series of terms in Eq. (7) for changes in vibrational quantum number $n \rightarrow n + 1$.

From the relation for the spectral emissivity given in Eq. (5), it follows that the total equilibrium intensity of radiation emitted per unit surface area per unit time into a solid angle of 2π steradians in the wave number interval between ν and $\nu + d\nu$ by heated gases distributed uniformly at an optical density of pL is:

$$J_\nu = J_\nu^0 [1 - e^{-P_\nu pL}] \quad (8)$$

Here J_ν^0 is the intensity of radiation emitted by a blackbody in the wave number interval between ν and $\nu + d\nu$ into a solid angle of 2π steradians per unit surface per unit time. The quantity J_ν^0 is obtained from Eq. (1) by multiplying by $c/4$. It is given analytically by the relation:

$$J_\nu^0 d\nu = c_1 \nu^5 [e^{c_2 \nu/T} - 1]^{-1} d\nu \quad (9)$$

where

ν = wave number (cm^{-1})

T = absolute temperature

$$c_1 = 2\pi c^2 h = 3.732 \times 10^{-5} \text{ erg} \cdot \text{cm}^2 \text{ sec}^{-1}$$

$$c_2 = ch/k = 1.432 \text{ cm} \cdot {}^\circ\text{K}$$

According to the Stephan-Boltzmann law, which is obtained by integrating Eq. (9) over the wave number interval from zero to infinity, the total energy emitted by a blackbody is proportional to the fourth power of the absolute temperature, i.e.,

$$\int_{\nu}^{\infty} J_{\nu} d\nu = \sigma T^4 \quad (10)$$

where σ is the Stephan-Boltzmann constant. The engineering definition of the overall emissivity is

$$\epsilon = \int_{-\infty}^{\infty} J_{\nu} d\nu / \sigma T^4 \quad (11)$$

Since the interest here is in comparing theoretical calculations with empirically determined (engineering) emissivities, further discussion will be restricted to Eq. (11).

The problem of emissivity calculations reduces to the evaluation of integrals of the type shown as Eq. (11). This integration can be accomplished if the width of the rotational lines is so small that they may be treated as being completely separated. This problem is considered in Section IV where it will be shown that the results obtained are applicable at moderate total pressures provided the optical densities are not too large. The integrals can also be evaluated approximately if the pressures are so high that extensive overlapping of the rotational

lines occurs. The pressures experienced in rocket combustion chambers are sufficiently high to justify a treatment based on extensive overlapping of rotational lines for many molecules.⁽⁷⁾ Calculations of the emissivities of gases at intermediate pressures and optical densities are more complicated as the result of partial overlapping of rotational lines.

III. BASIC NUMERICAL DATA

This section will be devoted to a compilation of the numerical data which are necessary for performing emissivity calculations.

A. Determination of Line Widths

The spectral line half-width α is defined as the frequency interval for which the absorption is greater than one-half its maximum value. The determination of its magnitude under different conditions of optical density, total pressure, and temperature is complicated by the number of influencing factors, such as Doppler broadening, collision broadening, Van der Waal's broadening, electric fields, etc. which effect its value. (13)

The natural half-width of the rotational lines is negligibly small. Available theoretical and experimental information^(4,13) indicates that the rotational lines of a simple diatomic molecule at moderate pressures may be considered to be composed primarily of the contributions resulting from Doppler and collision broadening.

The Doppler half-width of a rotational line is expressed by the relation⁽¹³⁾,

$$\alpha_d = (\log 2)^{\frac{1}{2}} (2RT/Mc^2)^{\frac{1}{2}} \nu_0 \quad (12)$$

where R is the gas constant per mole, M is the molecular weight of the emitting gas, and ν_0 is the wave number of the center of the rotational line.

The half-width α_c resulting from collision broadening can be obtained from the relation⁽¹³⁾,

$$\alpha_e = (1/\pi)(2\pi kT)^{1/2} n_p \rho^2 \left[(m_1 - m_2)/m_1 \right]^{1/2} \quad (13)$$

where ρ is the optical collision diameter which must be determined empirically, and m_1 and m_2 are the masses of the perturbing and absorbing molecules, respectively.

Reference to Eq. (12) indicates that the Doppler half-width can be determined without the use of experimental data. For the case of interest in connection with the present emissivity calculations, i.e., at temperatures of 300 and 500° K, the Doppler half-width is negligibly small compared to α_e . (For CO at 500° K with ν^0 equal to 2100 cm^{-1} it is found that $\alpha_d \sim 2.1 \times 10^{-3} \text{ cm}^{-1}$.)

It is evident that α_c cannot be calculated from Eq. (13) since ρ must be determined experimentally. For the present calculations, experimentally determined values of the rotational half-width will be used. It has been found⁽¹⁷⁾ that the rotational half-width for self-broadening of CO is $0.077 \text{ cm}^{-1} \text{ atm}^{-1}$. The calculations described in Section V indicate that this value for the rotational half-width leads to good agreement with the experimentally determined emissivities reported by Ullrich, who, however, performed his measurements on mixtures of CO and air. The rotational half-width for CO-air mixtures has not been measured. It is probably somewhat less than $0.077 \text{ cm}^{-1} \text{ atm}^{-1}$.

B. Calculation of Line Centers for Vibration-Rotation Transitions

According to the Bohr frequency rule, the transition between two non-degenerate stationary energy states E_i and E_j , where $E_i > E_j$, will be accompanied by the emission of radiant energy of the frequency:

$$\nu_{ij} = \frac{E_i - E_j}{hc} \quad (14)$$

where h is Planck's constant and c is the velocity of light. It is well known that the energy levels for a diatomic vibrating-rotating molecule can be expressed accurately⁽¹⁰⁾ by the relation

$$E(n, j) = (n + \frac{1}{2})hc \nu_e - (n + \frac{1}{2})^2 hc \chi_e \nu_e + j(j+1)hc B_e - j(j+1)^2 hc D_e - (n + \frac{1}{2})j(j+1)hc \alpha' \quad (15)$$

where

$$\nu^* = \nu_0 (1 - \chi_0) = \nu_e (1 - 2\chi_e)$$

$$\chi^* \nu^* = \chi_0 \nu_0 = \chi_e \nu_e$$

$$B_0 = B_e - \frac{1}{2}\alpha$$

$$\gamma = \frac{1}{2} \left(\frac{D_e}{B_e} \right)^{\frac{1}{2}} = B_e / \nu_e$$

$$\delta = \frac{\alpha}{B_e} = \left(\frac{6B_e}{\nu_e} \right) \left[\left(\frac{\chi_e \nu_e}{B_e} \right)^{\frac{1}{2}} - 1 \right]$$

The empirical constants for carbon monoxide are⁽¹⁰⁾

$$\nu^* = 2142.3 \text{ cm}^{-1}$$

$$B_0 = 1.916 \text{ cm}^{-1}$$

$$\chi^* = 0.00620$$

$$\chi_e = 0.006124$$

$$\gamma = 0.00394$$

$$\delta = 0.0091$$

$$\alpha = 3.199$$

The wave numbers of the spectral line centers associated with the

TABLE I

WAVE NUMBERS (cm^{-1}) CORRESPONDING TO ENERGY TRANSITIONS
FOR THE FUNDAMENTAL VIBRATION-ROTATION BAND OF CO

$$n \rightarrow n + 1, \Delta j = -1$$

$j \rightarrow j - 1$	$0 \rightarrow 1$	$1 \rightarrow 2$	$2 \rightarrow 3$	$3 \rightarrow 4$	$4 \rightarrow 5$	$5 \rightarrow 6$	$6 \rightarrow 7$
1 → 0	2138.4	2119.7	2085.4	2058.9	2032.4	2005.9	1979.3
2 → 1	2134.6	2108.1	2081.6	2055.1	2028.6	2002.1	1975.6
3 → 2	2130.6						
4 → 3	2126.6	2100.3	2073.8	2047.4	2021.0	1994.6	1968.1
5 → 4	2122.6						
6 → 5	2118.6	2092.3	2066.0	2039.6	2013.2	1986.9	1960.5
7 → 6	2114.5						
8 → 7	2110.4	2084.2	2057.9	2031.6	2005.4	1979.1	1952.8
9 → 8	2106.3						
10 → 9	2102.1	2076.0	2049.8	2023.5	1997.3	1971.1	1944.9
11 → 10	2097.9						
12 → 11	2093.6	2067.6	2041.5	2015.3	1989.2	1963.1	1936.8
13 → 12	2089.3						
14 → 13	2085.0	2059.1	2033.0	2006.9	1980.9	1954.8	1928.7
15 → 14	2080.7						
16 → 15	2076.3	2050.4	2024.5	1998.4	1972.4	1946.5	1920.4
17 → 16	2071.9						
18 → 17	2067.4	2041.7	2015.8	1989.8	1963.9	1938.0	1912.0
19 → 18	2063.0						
20 → 19	2058.4	2032.8	2006.9	1981.0	1955.2	1929.4	1903.4
22 → 21	2049.3	2023.8	1998.0	1972.2	1946.4	1920.6	1894.8
24 → 23	2040.1	2014.6	1988.9	1963.1	1937.4	1911.8	1885.9
26 → 25	2030.6	2005.3	1979.7	1954.0	1928.4	1902.8	1877.0
28 → 27	2021.1	1995.9	1970.3	1944.7	1919.2	1893.6	1867.9
30 → 29	2011.5	1986.4	1960.9	1935.3	1909.9	1884.4	1858.8
32 → 31	2001.7	1976.7	1951.3	1927.3	1900.4	1875.0	1849.5
34 → 33	1991.8	1967.0	1941.6	1916.1	1890.8	1865.5	1840.0
36 → 35	1981.3	1957.1	1931.7	1906.4	1881.2	1855.9	1830.5
38 → 37	1971.7	1947.0	1921.8	1896.5	1871.4	1846.2	1820.8
40 → 39	1961.4	1936.9	1911.7	1886.5	1861.4	1836.3	1811.0
42 → 41	1951.0	1926.7	1901.6	1876.4	1851.4	1826.3	1801.1
44 → 43	1940.5	1916.3	1891.3	1866.1	1841.2	1816.2	1791.1
46 → 45	1929.9	1905.8	1880.8	1855.8	1831.0	1806.0	1780.9
48 → 47	1919.1	1895.2	1870.3	1845.3	1820.6	1795.7	1770.7
50 → 49	1908.3	1884.5	1859.7	1834.7	1810.1	1785.3	1760.3

TABLE I (CONTINUED)

$j \rightarrow j - 1$	$0 \rightarrow 1$	$1 \rightarrow 2$	$2 \rightarrow 3$	$3 \rightarrow 4$	$4 \rightarrow 5$	$5 \rightarrow 6$	$6 \rightarrow 7$
52 → 51	1897.3	1873.7	1848.9	1824.0	1799.5	1774.8	1749.8
54 → 53	1886.2	1862.7	1838.1	1813.2	1788.7	1764.1	1739.2
56 → 55	1875.0	1851.7	1827.1	1802.3	1777.9	1753.4	1728.5
58 → 57	1863.8	1840.6	1816.0	1791.3	1767.0	1742.5	1717.7
60 → 59	1852.3	1829.3	1804.8	1780.2	1755.9	1731.5	1706.8
62 → 61	1840.8	1817.9	1793.5	1769.0	1744.8	1720.4	1695.8
64 → 63	1829.2	1806.5	1782.1	1757.6	1733.5	1709.3	1684.7
66 → 65	1817.5	1794.9	1770.6	1746.2	1722.2	1698.0	1673.4
68 → 67	1805.6	1783.2	1759.0	1734.6	1710.7	1686.6	1662.1
70 → 69	1793.6	1771.5	1747.4	1723.0	1699.2	1675.1	1650.7
72 → 71	1781.6	1759.6	1735.6	1711.3	1676.9	1663.5	1639.2
74 → 73	1769.5	1757.7	1723.7	1699.4	1675.8	1651.8	1627.5
76 → 75	1757.2	1735.6	1711.7	1687.4	1663.9	1640.0	1615.8
78 → 77	1744.9	1723.4	1699.6	1675.4	1652.0	1628.2	1604.0
80 → 79	1732.4	1711.2	1687.4	1663.3	1639.9	1616.2	1592.1
82 → 81	1719.9	1698.8	1675.1	1651.1	1627.8	1604.1	1580.1
84 → 83	1707.2	1686.4	1662.7	1638.8	1615.5	1592.0	1566.0
86 → 85	1694.5	1673.8	1650.3	1626.4	1603.2	1579.7	1555.8
88 → 87	1681.7	1661.2	1637.7	1613.8	1590.8	1567.4	1543.5
90 → 89	1668.8	1648.5	1625.1	1601.3	1578.3	1555.0	1531.1
92 → 91	1655.8	1635.7	1612.4	1588.6	1565.7	1542.5	1518.6
94 → 93	1642.7	1622.8	1599.6	1575.8	1553.1	1529.9	1506.1
96 → 95	1629.5	1609.9	1586.7	1563.0	1540.3	1517.2	1493.5
98 → 97	1616.2	1596.8	1573.7	1550.1	1527.5	1504.4	1480.7
100 → 99	1602.9	1583.7	1560.6	1537.1	1514.6	1490.8	1467.9
105 → 104	1569.1	1550.5	1527.6	1504.2	1481.9	1459.1	1435.6
110 → 109	1534.9	1516.8	1494.1	1470.8	1448.7	1426.1	1402.7
115 → 114	1500.1	1482.7	1460.1	1436.8	1415.1	1392.6	1369.4
120 → 119	1464.9	1448.1	1425.7	1402.6	1381.1	1358.8	1335.6
125 → 124	1429.2	1413.0	1390.8	1367.9	1346.5	1324.4	1301.4
130 → 129	1393.1	1377.6	1355.6	1332.7	1311.6	1289.7	1266.8

TABLE II

WAVE NUMBERS (cm^{-1}) CORRESPONDING TO ENERGY TRANSITIONS
FOR THE FUNDAMENTAL VIBRATION-ROTATION BAND OF CO

$$n \rightarrow n + 1, \Delta j = +1$$

$j - 1 \rightarrow j$	$0 \rightarrow 1$	$1 \rightarrow 2$	$2 \rightarrow 3$	$3 \rightarrow 4$	$4 \rightarrow 5$	$5 \rightarrow 6$	$6 \rightarrow 7$
0 → 1	2146.1	2119.6	2093.0	2066.4	2039.8	2013.2	1986.5
1 → 2	2149.9	2123.3	2096.7	2070.0	2043.4	2016.8	1990.1
2 → 3	2153.7						
3 → 4	2157.4	2130.7	2104.0	2077.3	2050.6	2023.9	1997.2
4 → 5	2161.1						
5 → 6	2164.7	2138.0	2111.2	2084.4	2057.6	2030.9	2004.1
6 → 7	2168.3						
7 → 8	2171.9	2145.1	2118.2	2091.4	2064.5	2037.7	2010.8
8 → 9	2175.4						
9 → 10	2178.9	2152.1	2125.1	2098.2	2071.3	2044.4	2017.4
10 → 11	2182.4						
11 → 12	2185.8	2156.9	2131.9	2104.9	2077.9	2051.0	2023.9
12 → 13	2189.2						
13 → 14	2192.5	2165.6	2138.5	2111.4	2084.4	2057.3	2030.2
14 → 15	2195.8						
15 → 16	2199.1	2172.1	2144.9	2117.8	2090.7	2063.6	2036.4
16 → 17	2202.3						
17 → 18	2205.5	2178.5	2151.2	2124.0	2096.8	2069.7	2042.4
18 → 19	2208.7						
19 → 20	2211.8	2184.7	2157.4	2130.1	2102.9	2075.6	2048.3
21 → 22	2217.9	2190.8	2163.4	2136.0	2108.7	2081.4	2054.0
23 → 24	2223.9	2196.7	2169.2	2141.8	2114.4	2087.0	2059.5
25 → 26	2229.7	2202.4	2174.9	2147.4	2120.0	2092.5	2064.9
27 → 28	2235.3	2208.0	2180.5	2152.8	2125.3	2097.3	2070.2
29 → 30	2240.8	2213.5	2185.8	2158.1	2130.6	2103.0	2075.5
31 → 32	2246.1	2218.8	2191.1	2163.3	2135.7	2108.0	2080.2
33 → 34	2251.3	2223.9	2196.1	2168.2	2140.6	2112.3	2085.0
35 → 36	2256.3	2228.9	2201.0	2173.1	2145.3	2117.5	2089.2
37 → 38	2261.1	2233.7	2205.7	2177.7	2149.9	2122.0	2094.0
39 → 40	2265.8	2238.3	2210.3	2182.2	2154.3	2126.4	2098.3
41 → 42	2270.3	2242.8	2214.7	2186.5	2158.6	2130.6	2102.4
43 → 44	2274.6	2247.1	2218.9	2190.7	2162.7	2134.6	2106.3
45 → 46	2278.8	2251.2	2223.0	2194.7	2166.6	2136.5	2110.1
47 → 48	2282.7	2255.2	2226.9	2198.5	2170.4	2142.2	2113.7
49 → 50	2286.6	2259.0	2230.6	2202.2	2174.0	2145.7	2117.2

TABLE II (CONTINUED)

$j - 1 \rightarrow j$	$0 \rightarrow 1$	$1 \rightarrow 2$	$2 \rightarrow 3$	$3 \rightarrow 4$	$4 \rightarrow 5$	$5 \rightarrow 6$	$6 \rightarrow 7$
51 → 52	2290.2	2262.6	2234.2	2205.6	2177.4	2149.0	2120.4
53 → 54	2293.7	2266.1	2238.0	2209.0	2180.7	2152.2	2123.5
55 → 56	2296.9	2269.4	2240.8	2212.1	2183.7	2155.2	2126.5
57 → 58	2300.1	2272.5	2243.9	2215.1	2186.6	2158.1	2129.2
59 → 60	2303.0	2275.4	2246.7	2217.8	2189.4	2160.9	2131.5
61 → 62	2305.7	2278.2	2249.4	2220.5	2191.9	2163.2	2134.2
63 → 64	2308.3	2280.8	2251.9	2222.9	2194.3	2165.5	2136.4
65 → 66	2310.7	2283.2	2254.3	2225.1	2196.5	2167.6	2138.4
67 → 68	2312.9	2285.4	2256.4	2227.2	2198.5	2169.5	2140.3
69 → 70	2315.0	2287.4	2258.4	2229.1	2200.3	2171.3	2142.0
71 → 72	2316.8	2289.5	2260.2	2230.8	2202.0	2172.9	2143.4
73 → 74	2318.5	2291.0	2261.8	2232.3	2203.4	2174.3	2144.8
75 → 76	2319.9	2292.5	2263.2	2233.6	2204.7	2175.5	2145.9
77 → 78	2321.3	2293.8	2264.4	2234.8	2205.8	2176.5	2146.8
79 → 80	2322.3	2294.9	2265.5	2235.8	2206.7	2177.3	2147.6
81 → 82	2323.2	2295.8	2266.3	2236.8	2207.4	2178.0	2148.1
83 → 84	2323.9	2296.6	2267.0	2237.1	2207.9	2178.5	2148.5
85 → 86	2324.5	2297.1	2267.5	2237.5	2208.3	2178.7	2148.7
87 → 88	2324.8	2297.5	2267.8	2237.7	2208.4	2178.8	2148.7
89 → 90	2324.9	2297.6	2267.9	2237.7	2208.4	2178.7	2148.5
91 → 92	2324.8	2297.6	2267.8	2237.5	2208.1	2178.4	2148.1
93 → 94	2324.6	2297.3	2267.5	2237.1	2207.7	2177.8	2147.5
95 → 96	2324.1	2296.9	2267.0	2236.5	2207.1	2177.1	2146.7
97 → 98	2323.4	2296.3	2266.3	2235.8	2206.2	2176.2	2145.7
99 → 100	2322.6	2295.5	2265.4	2234.8	2205.2	2175.1	2144.5
104 → 105	2319.5	2292.6	2262.3	2231.4	2201.7	2171.5	2140.6
109 → 110	2315.1	2288.4	2257.9	2226.8	2197.0	2166.6	2135.5
114 → 115	2309.5	2282.9	2252.2	2220.9	2191.0	2160.4	2129.0
119 → 120	2302.5	2276.0	2245.2	2213.9	2183.6	2152.9	2121.3
124 → 125	2294.2	2267.9	2236.9	2205.2	2175.0	2144.0	2112.2
129 → 130	2284.5	2253.4	2227.3	2195.2	2165.0	2133.8	2101.8

TABLE III

WAVE NUMBERS (cm^{-1}) CORRESPONDING TO ENERGY TRANSITIONS
FOR THE VIBRATION-ROTATION BAND OF THE FIRST OVERTONE OF CO

$$n \rightarrow n + 2, \Delta j = -1$$

$J \rightarrow J - 1$	$0 \rightarrow 2$	$1 \rightarrow 3$	$2 \rightarrow 4$	$3 \rightarrow 5$	$4 \rightarrow 6$	$5 \rightarrow 7$
1 → 0	4254.2	4201.1	4148.0	4094.9	4041.9	3988.8
2 → 1	4250.3	4197.2	4144.1	4091.1	4038.1	3985.0
3 → 2						
4 → 3	4212.2	4189.2	4136.2	4083.5	4030.3	3977.3
5 → 4						
6 → 5	4233.9	4180.9	4128.0	4075.1	4022.3	3969.4
7 → 6						
8 → 7	4225.2	4172.4	4119.5	4066.7	4013.9	3961.0
9 → 8						
10 → 9	4216.3	4163.6	4110.7	4053.0	4005.3	3952.5
11 → 10						
12 → 11	4207.1	4154.4	4101.7	4049.0	3996.4	3943.6
13 → 12						
14 → 13	4197.6	4145.0	4092.4	4039.8	3987.3	3934.5
15 → 14						
16 → 15	4187.9	4135.4	4082.7	4030.3	3977.8	3925.2
17 → 16						
18 → 17	4177.9	4125.4	4072.9	4020.4	3968.0	3915.5
19 → 18						
20 → 19	4167.6	4115.2	4062.8	4010.4	3958.1	3905.6
22 → 21	4157.0	4104.8	4052.3	4000.0	3947.8	3895.4
24 → 23	4146.2	4094.0	4041.7	3989.4	3937.4	3884.9
26 → 25	4135.0	4083.0	4030.7	3978.6	3926.5	3874.2
28 → 27	4123.7	4071.8	4019.5	3967.4	3915.4	3863.2
30 → 29	4112.0	4060.2	4008.0	3956.0	3904.0	3851.9
32 → 31	4100.1	4048.4	3996.3	3944.4	3892.5	3840.4
34 → 33	4087.9	4036.4	3984.3	3932.4	3880.6	3828.6
36 → 35	4075.5	4024.0	3972.0	3920.2	3868.5	3816.6
38 → 37	4062.8	4011.4	3959.5	3907.8	3856.1	3804.2
40 → 39	4049.8	3998.6	3946.7	3895.0	3843.5	3791.6
42 → 41	4036.6	3985.4	3933.7	3882.0	3830.6	3778.8
44 → 43	4022.1	3972.0	3920.4	3868.8	3817.4	3765.7
46 → 45	4007.8	3958.4	3906.8	3855.4	3804.0	3752.4
48 → 47	3995.3	3944.6	3893.0	3841.6	3790.4	3738.8
50 → 49	3981.1	3930.4	3879.0	3827.6	3776.4	3724.9

TABLE III (CONTINUED)

$j \rightarrow j - 1$	$0 \rightarrow 2$	$1 \rightarrow 3$	$2 \rightarrow 4$	$3 \rightarrow 5$	$4 \rightarrow 6$	$5 \rightarrow 7$
52 → 51	3966.6	3916.0	3864.6	3813.4	3762.3	3710.8
54 → 53	3951.8	3901.4	3850.1	3798.9	3747.8	3696.4
56 → 55	3936.8	3886.6	3835.2	3784.1	3733.2	3681.8
58 → 57	3921.5	3871.4	3820.2	3769.1	3718.3	3667.0
60 → 59	3906.0	3856.0	3804.8	3753.9	3703.1	3651.9
62 → 61	3890.2	3840.4	3789.3	3738.4	3687.7	3636.5
64 → 63	3874.2	3824.6	3773.5	3722.6	3672.0	3620.9
66 → 65	3857.9	3808.4	3757.4	3706.6	3656.1	3605.1
68 → 67	3841.4	3792.1	3741.1	3690.4	3640.0	3589.0
70 → 69	3824.7	3775.5	3724.5	3673.9	3623.6	3572.6
72 → 71	3807.7	3758.7	3707.8	3657.2	3607.5	3556.1
74 → 73	3790.4	3741.6	3690.8	3643.3	3590.1	3539.3
76 → 75	3773.0	3724.2	3673.5	3623.1	3573.0	3522.2
78 → 77	3755.2	3706.8	3656.0	3605.6	3555.7	3505.0
80 → 79	3737.2	3688.9	3638.3	3588.0	3538.1	3487.4
82 → 81	3719.2	3670.9	3620.3	3570.1	3520.3	3469.7
84 → 83	3700.7	3652.6	3602.1	3552.0	3502.3	3451.7
86 → 85	3682.0	3634.2	3583.7	3533.6	3484.0	3433.5
88 → 87	3663.2	3615.4	3565.0	3515.0	3465.4	3415.0
90 → 89	3644.0	3596.5	3546.1	3496.2	3446.7	3396.3
92 → 91	3624.6	3577.4	3527.0	3477.1	3427.7	3377.4
94 → 93	3605.1	3562.0	3507.7	3457.8	3408.6	3358.3
96 → 95	3585.3	3538.3	3488.1	3438.4	3389.2	3338.9
98 → 97	3565.2	3518.4	3468.3	3418.6	3369.5	3319.4
100 → 99	3544.9	3498.4	3448.3	3398.7	3349.6	3299.5
105 → 104	3493.3	3447.2	3397.2	3347.8	3299.0	3249.0
110 → 109	3440.3	3394.7	3344.8	3295.6	3247.0	3197.1
115 → 114	3385.9	3340.8	3291.0	3242.0	3193.6	3143.9
120 → 119	3330.1	3285.6	3236.0	3187.1	3139.0	3089.3
125 → 124	3273.0	3229.0	3179.5	3130.8	3082.9	3033.4
130 → 129	3214.6	3171.2	3121.8	3073.3	3025.6	2976.3

TABLE IV

WAVE NUMBERS (cm^{-1}) CORRESPONDING TO ENERGY TRANSITIONS
FOR THE VIBRATION-ROTATION BAND OF THE FIRST OVERTONE OF CO

$$n \rightarrow n + 2, \Delta j = +1$$

$J - 1 \rightarrow J$	$0 \rightarrow 2$	$1 \rightarrow 3$	$2 \rightarrow 4$	$3 \rightarrow 5$	$4 \rightarrow 6$	$5 \rightarrow 7$
0 → 1	4261.8	4206.6	4155.5	4102.3	4049.3	3996.1
1 → 2	4265.6	4212.4	4159.1	4106.0	4052.8	3996.6
2 → 3						
3 → 4	4272.8	4219.6	4166.2	4113.0	4059.8	4006.5
4 → 5						
5 → 6	4279.7	4226.4	4173.0	4119.7	4066.4	4013.0
6 → 7						
7 → 8	4286.4	4233.0	4179.6	4126.2	4072.8	4021.3
8 → 9						
9 → 10	4292.8	4239.2	4185.8	4132.3	4078.9	4025.4
10 → 11						
11 → 12	4298.6	4245.3	4191.7	4138.2	4084.7	4031.1
12 → 13						
13 → 14	4301.1	4251.0	4197.3	4143.7	4090.2	4036.6
14 → 15						
15 → 16	4304.6	4256.4	4202.7	4149.0	4095.4	4041.7
16 → 17						
17 → 18	4315.3	4261.6	4207.8	4154.0	4100.3	4046.5
18 → 19						
19 → 20	4320.2	4266.4	4212.5	4158.7	4105.0	4051.1
21 → 22	4324.7	4271.0	4217.0	4163.2	4109.3	4055.4
23 → 24	4329.1	4275.2	4221.2	4167.2	4113.4	4059.4
25 → 26	4333.0	4279.2	4225.1	4171.1	4117.1	4063.0
27 → 28	4336.8	4282.8	4228.7	4174.6	4120.6	4066.4
29 → 30	4340.2	4286.2	4232.0	4177.8	4123.7	4069.5
31 → 32	4342.9	4289.3	4234.9	4180.7	4126.6	4072.2
33 → 34	4346.1	4292.0	4237.7	4183.4	4129.1	4074.9
35 → 36	4348.5	4294.5	4240.0	4185.7	4131.4	4076.9
37 → 38	4350.8	4296.6	4242.1	4187.7	4133.3	4078.8
39 → 40	4352.6	4298.6	4243.9	4189.4	4135.0	4080.3
41 → 42	4354.2	4300.1	4245.4	4190.3	4136.2	4081.6
43 → 44	4354.5	4301.3	4246.5	4191.9	4137.3	4082.5
45 → 46	4356.4	4302.2	4247.4	4192.7	4138.0	4083.2
47 → 48	4357.1	4302.9	4247.9	4193.1	4138.5	4083.5
49 → 50	4357.4	4303.2	4248.1	4193.3	4138.6	4083.5

TABLE IV (CONTINUED)

$j - 1 \rightarrow j$	$0 \rightarrow 2$	$1 \rightarrow 3$	$2 \rightarrow 4$	$3 \rightarrow 5$	$4 \rightarrow 6$	$5 \rightarrow 7$
51 → 52	4357.4	4303.2	4248.1	4193.1	4138.4	4083.2
53 → 54	4357.1	4302.9	4247.7	4192.7	4137.8	4082.6
55 → 56	4356.4	4302.2	4247.0	4191.9	4137.0	4081.7
57 → 58	4355.5	4301.3	4246.0	4190.8	4135.9	4080.5
59 → 60	4354.3	4300.1	4244.6	4189.4	4134.4	4079.0
61 → 62	4352.7	4298.5	4242.9	4187.7	4132.6	4077.1
63 → 64	4350.8	4296.6	4241.0	4185.6	4130.5	4074.9
65 → 66	4348.5	4294.4	4238.7	4183.2	4128.1	4072.4
67 → 68	4346.0	4291.8	4236.0	4180.6	4125.3	4069.5
69 → 70	4343.2	4289.0	4233.1	4177.6	4122.3	4066.4
71 → 72	4339.9	4285.8	4229.9	4174.2	4118.4	4062.9
73 → 74	4336.4	4282.3	4226.3	4170.6	4115.1	4059.1
75 → 76	4332.6	4278.5	4222.4	4166.6	4111.1	4055.0
77 → 78	4328.4	4274.3	4218.1	4162.3	4106.7	4050.6
79 → 80	4323.9	4269.8	4213.5	4157.6	4102.0	4045.8
81 → 82	4319.0	4265.0	4208.6	4152.6	4097.0	4040.6
83 → 84	4313.9	4259.8	4203.4	4147.4	4091.7	4035.2
85 → 86	4308.2	4254.4	4197.8	4141.7	4085.9	4029.4
87 → 88	4302.5	4248.6	4191.9	4135.7	4080.0	4023.3
89 → 90	4296.3	4242.4	4185.7	4129.4	4073.6	4016.9
91 → 92	4289.8	4236.0	4179.1	4122.8	4066.9	4010.1
93 → 94	4282.9	4229.1	4172.2	4115.8	4059.8	4003.0
95 → 96	4275.9	4222.0	4165.0	4108.5	4052.5	3995.5
97 → 98	4268.2	4214.5	4157.4	4100.8	4044.8	3937.7
99 → 100	4260.3	4206.6	4149.4	4092.8	4036.8	3979.6
104 → 105	4239.1	4185.6	4128.2	4071.3	4015.2	3957.7
109 → 110	4215.7	4162.4	4104.7	4047.7	3991.4	3933.8
114 → 115	4190.2	4136.9	4079.0	4021.9	3965.4	3907.6
119 → 120	4162.4	4109.4	4051.2	3993.9	3937.3	3879.2
124 → 125	4132.4	4079.5	4021.2	3963.6	3906.9	3848.6
129 → 130	4100.1	4047.4	3983.9	3931.2	3874.4	3810.3

TABLE V

WAVE NUMBERS (cm^{-1}) CORRESPONDING TO ENERGY TRANSITIONS
FOR THE VIBRATION-ROTATION BAND OF THE SECOND OVERTONE OF CO

$$n \rightarrow n + 3, \Delta j = -1$$

$j \rightarrow j - 1$	$0 \rightarrow 3$	$1 \rightarrow 4$	$2 \rightarrow 5$	$3 \rightarrow 6$
1 → 0	6343.4	6263.7	6184.0	6104.4
2 → 1	6339.5	6259.8	6180.1	6100.6
4 → 3	6331.2	6251.7	6172.0	6092.6
6 → 5	6322.5	6243.1	6163.6	6084.1
8 → 7	6313.4	6234.0	6154.6	6075.3
10 → 9	6303.9	6224.6	6145.2	6065.9
12 → 11	6293.9	6214.8	6135.4	6056.2
14 → 13	6283.6	6204.5	6125.2	6046.1
16 → 15	6272.9	6193.8	6114.6	6035.6
18 → 17	6261.6	6182.7	6103.6	6024.6
20 → 19	6250.0	6171.2	6092.2	6013.2
22 → 21	6238.0	6159.2	6000.2	6001.5
24 → 23	6225.6	6146.9	6068.0	5989.3
26 → 25	6212.8	6134.2	6055.4	5976.7
28 → 27	6199.5	6121.0	6042.3	5963.6
30 → 29	6185.9	6107.5	6023.8	5950.2
32 → 31	6171.8	6093.5	6014.9	5936.4
34 → 33	6157.3	6079.1	6000.6	5922.2
36 → 35	6142.5	6064.4	5985.9	5907.6
38 → 37	6127.2	6049.2	5970.8	5892.6
40 → 39	6111.5	6033.6	5955.3	5877.1
42 → 41	6095.4	6017.7	5939.4	5861.3
44 → 43	6078.9	6001.3	5923.1	5845.1
46 → 45	6062.1	5984.5	5901.6	5828.4
48 → 47	6044.7	5967.4	5883.8	5811.4
50 → 49	6027.1	5949.8	5871.8	5794.0
52 → 51	6009.0	5931.9	5854.0	5776.2
54 → 53	5990.5	5913.5	5835.7	5758.0
56 → 55	5971.7	5894.8	5817.0	5739.4
58 → 57	5952.5	5875.6	5798.0	5720.4
60 → 59	5932.8	5856.2	5773.5	5701.0
62 → 61	5912.7	5836.2	5758.6	5681.3
64 → 63	5892.4	5816.0	5738.6	5661.1
66 → 65	5871.5	5795.3	5717.9	5640.6
68 → 67	5850.3	5774.2	5696.9	5619.7
70 → 69	5828.6	5752.8	5675.5	5598.4

TABLE V (CONTINUED)

$J \rightarrow J - 1$	$0 \rightarrow 3$	$1 \rightarrow 4$	$2 \rightarrow 5$	$3 \rightarrow 6$
72 → 71	5806.8	5730.9	5653.8	5576.7
74 → 73	5784.5	5708.7	5631.6	5554.6
76 → 75	5761.7	5686.2	5609.2	5532.2
78 → 77	5738.6	5663.2	5586.3	5509.4
80 → 79	5715.1	5639.9	5563.0	5486.2
82 → 81	5691.3	5616.2	5539.4	5462.6
84 → 83	5667.0	5592.1	5515.3	5438.7
86 → 85	5642.4	5567.6	5491.0	5414.3
88 → 87	5617.4	5542.8	5466.2	5389.7
90 → 89	5592.0	5517.6	5441.0	5364.6
92 → 91	5566.3	5492.0	5415.5	5339.2
94 → 93	5540.2	5466.1	5389.7	5313.4
96 → 95	5513.8	5439.8	5363.4	5287.2
98 → 97	5486.9	5413.1	5336.8	5260.7
100 → 99	5459.7	5386.1	5309.9	5233.8
105 → 104	5390.1	5316.9	5240.8	5165.0
110 → 109	5318.2	5245.5	5169.6	5093.9
115 → 114	5244.1	5171.8	5096.2	5020.6
120 → 119	5167.7	5095.9	5020.4	4945.0
125 → 124	5089.1	5017.8	4942.5	4867.2
130 → 129	5008.4	4937.5	4862.4	4787.3

TABLE VI

WAVE NUMBERS (cm^{-1}) CORRESPONDING TO ENERGY TRANSITIONS
FOR THE VIBRATION-ROTATION BAND OF THE SECOND OVERTONE OF CO

$$n \rightarrow n + 3, \Delta j = +1$$

$j - 1 \rightarrow j$	$0 \rightarrow 3$	$1 \rightarrow 4$	$2 \rightarrow 5$	$3 \rightarrow 6$
0 → 1	6351.0	6271.3	6191.6	6111.8
1 → 2	6354.7	6274.9	6195.1	6115.4
3 → 4	6361.7	6281.9	6202.0	6122.2
5 → 6	6368.2	6288.3	6203.4	6123.5
7 → 8	6374.2	6294.4	6214.4	6134.4
9 → 10	6380.0	6300.0	6219.9	6140.4
11 → 12	6385.3	6305.2	6225.0	6145.1
13 → 14	6390.2	6309.9	6229.7	6149.8
15 → 16	6394.5	6314.3	6234.0	6154.0
17 → 18	6398.4	6318.2	6237.8	6157.9
19 → 20	6401.9	6321.6	6241.2	6161.3
21 → 22	6405.0	6324.7	6244.2	6164.3
23 → 24	6407.7	6327.3	6246.7	6166.9
25 → 26	6409.9	6329.4	6248.8	6169.1
27 → 28	6411.7	6331.2	6250.4	6170.9
29 → 30	6412.9	6332.4	6251.6	6172.3
32 → 32	6413.8	6333.3	6252.4	6173.3
33 → 34	6414.3	6333.7	6252.8	6173.9
35 → 36	6414.3	6333.6	6252.6	6174.0
37 → 38	6413.8	6333.1	6252.0	6173.8
39 → 40	6412.9	6332.2	6251.0	6173.2
41 → 42	6411.6	6330.8	6249.6	6172.2
43 → 44	6409.7	6329.0	6247.7	6170.8
45 → 46	6407.5	6326.7	6245.4	6168.9
47 → 48	6404.8	6324.0	6242.5	6166.7
49 → 50	6401.6	6320.8	6239.2	6164.1
51 → 52	6398.0	6317.1	6235.6	6161.1
53 → 54	6393.9	6313.0	6231.4	6157.7
55 → 56	6389.4	6308.5	6226.8	6153.9
57 → 58	6384.4	6303.5	6221.8	6149.7
59 → 60	6378.9	6298.0	6216.2	6145.2
61 → 62	6373.0	6292.1	6210.2	6140.2
63 → 64	6366.6	6285.7	6203.7	6134.8
65 → 66	6359.9	6278.9	6196.9	6129.1
67 → 68	6352.6	6271.6	6189.4	6123.0
69 → 70	6344.7	6263.8	6181.6	6116.5

TABLE VI (CONTINUED)

$j - 1 \rightarrow j$	$0 \rightarrow 3$	$1 \rightarrow 4$	$2 \rightarrow 5$	$3 \rightarrow 6$
71 → 72	6336.5	6255.6	6173.3	6109.7
73 → 74	6327.8	6246.9	6164.6	6102.4
75 → 76	6318.7	6237.7	6155.3	6094.8
77 → 78	6309.0	6228.1	6145.6	6086.8
79 → 80	6298.9	6218.0	6135.4	6078.4
81 → 82	6288.3	6207.4	6124.8	6069.6
83 → 84	6277.2	6196.3	6113.6	6060.4
85 → 86	6265.7	6184.8	6102.0	6051.0
87 → 88	6253.7	6172.8	6090.0	6041.1
89 → 90	6241.2	6160.3	6077.4	6030.8
91 → 92	6228.3	6147.4	6064.4	6020.2
93 → 94	6214.8	6134.0	6051.0	6009.2
95 → 96	6200.9	6120.1	6037.0	5997.8
97 → 98	6186.5	6105.7	6022.4	5986.1
99 → 100	6171.6	6090.8	6007.6	5974.0
104 → 105	6132.4	6051.5	5968.1	5942.2
109 → 110	6039.8	6009.2	5925.6	5908.1
114 → 115	6044.3	5963.8	5830.1	5371.8
119 → 120	5995.7	5915.4	5831.4	5833.3
124 → 125	5914.1	5863.8	5779.7	5792.5
129 → 130	5839.3	5809.2	5724.9	5749.6

energy transitions $E_j^n \rightarrow E_{j+1}^{n+1}$, $E_j^n \rightarrow E_{j+1}^{n+2}$, and $E_j^n \rightarrow E_{j+1}^{n+3}$ (the fundamental and first and second overtones) for carbon monoxide are listed in Tables I - VI, inc.

C. Numerical Calculation of Integrated Absorption of Rotational Lines

The following outline for the calculation of integrated absorption for general vibrating-rotating diatomic molecules is valid for emitters which are in thermodynamic equilibrium.

The integrated absorptions for transitions from the ground vibrational level for the rotational lines of a diatomic molecule, in the region of the fundamental vibration-rotation spectrum is given by Oppenheimer's equation (14).

$$S_{j+j-1}^{o+1} = \frac{N_r \pi \epsilon^2}{3\mu c} \frac{\nu_{j+j-1}^{o+1}}{\nu_{o+1}} \frac{j \exp[-E_{o,j}/kT]}{\sum_n \sum_j (2j+1) \exp[-E_{n,j}/kT]} \quad F.G. \quad (16)$$

and

$$S_{j-1+j}^{o+1} = \frac{N_r \pi \epsilon^2}{3\mu c} \frac{\nu_{j-1+j}^{o+1}}{\nu_{o+1}} \frac{j \exp[-E_{o,j-1}/kT]}{\sum_n \sum_j (2j+1) \exp[-E_{n,j-1}/kT]} \quad F.G.' \quad (17)$$

The various symbols have the following meaning:

N_p = number of emitting molecules per unit volume per unit of total pressure

μ = reduced mass of carbon monoxide

ϵ = effective charge (esu) which must be determined empirically

c = velocity of light

$E_{n,j}$ = energy of the n^{th} vibrational and j^{th} rotational level, an explicit expression for which was given previously

$\nu_{0 \rightarrow 1}$ = wave number (cm^{-1}) corresponding to the (forbidden) transition $j = 0 \rightarrow j = 0$ and $n = 0 \rightarrow n = 1$

$\gamma_{j \rightarrow j' n \rightarrow n'}$ = wave number for the rotational transition $j \rightarrow j'$ and the vibrational transition $n \rightarrow n'$

T = temperature in $^{\circ}\text{K}$

k = the Boltzmann constant = 1.38048×10^{-16} erg/ $^{\circ}\text{K}$

h = Planck's constant = 6.6242×10^{-27} erg-sec

I = moment of inertia of the emitting molecule

= $h^2/8\sigma T \pi^2 k$ and $\sigma T = 2.743$ degrees for carbon monoxide

$$F = 1 + 4\gamma_j \left(1 + \frac{5\gamma_j}{8} - \frac{3\gamma}{8} \right)$$

$$F' = 1 - 4\gamma_j \left(1 - \frac{5\gamma_j}{8} - \frac{3\gamma}{8} \right)$$

$$G = 1 - \exp - \left(\frac{hc \nu_{j \rightarrow j-1}^0}{kT} \right)$$

$$G' = 1 - \exp - \left(\frac{hc \nu_{j-1 \rightarrow j}^0}{kT} \right)$$

$$\gamma = h/4\pi^2 I \nu_{0 \rightarrow 1} = 2.3116 \times 10^7.$$

As is discussed in more detail in Section D, the term

$\sum_n \sum_j (2j+1) \exp - (E_n, j/kT)$ represents the complete partition function and can be evaluated by standard statistical methods. If this term is represented by Q_{vjm} , then Eq. (16) and (17) can be written as:

$$S_{j \rightarrow j-1}^{0 \rightarrow 1} = \left(\frac{N_T \pi e^2}{3 \mu c Q_{vjm}} \right) \left(\frac{\nu_{j \rightarrow j-1}^{0 \rightarrow 1}}{\nu_{0 \rightarrow 1}} j \left[\exp - \left(\frac{E_{0,j}}{kT} \right) \right] F.G. \right) \quad (18)$$

and

$$S_{j-1 \rightarrow j}^{o+1} = \left(\frac{N_r \pi \epsilon^2}{3 \mu c Q_{vjm}} \right) \left(\frac{V_{j-1 \rightarrow j}^{o+1}}{V_{o+1}} j \left[\exp(-E_{o+1}/kT) \right] F' G' \right) \quad (19)$$

respectively.

The term in the first bracket of Eqs. (18) and (19) is temperature-dependent because both N_r and Q_{vjm} vary with temperature. The effective charge ϵ is presumably a constant. It has been determined empirically and has the value 3.14×10^{-10} electrostatic units.⁽¹⁷⁾ Assuming the validity of the ideal gas law, it is found for carbon monoxide at 300°K that

$$\frac{N_r \pi \epsilon^2}{3 \mu c^2} = 246.904 \text{ atmos}^{-1} \text{ cm}^{-2}$$

or

$$\frac{N_r \pi \epsilon^2}{3 \mu c} = 7.40144 \times 10^{12} (\text{cm-sec-atmos})^{-1}$$

Using the listed numerical value for $N_r \pi \epsilon^2 / 3 \mu c$, it is a simple matter to determine the value of $\beta = N_r \pi \epsilon^2 / 3 \mu c^2 Q_{vjm}$ by calculating Q_{vjm} according to the method described in Section III.D. In particular, at 300°K, it will be shown (Cf. Section III.D) that

$$Q_{vjm} = 0.66122$$

whence it follows that

$$\frac{N_r \pi \epsilon^2}{3 \mu c^2 Q_{vjm}} = 373.4 \text{ cm}^{-2} \text{ atmos}^{-1}$$

Referring to Eqs. (18) and (19), it is apparent that the terms in the second brackets are also dependent on the temperature but do not depend upon the effective charge and therefore can be calculated

accurately without requiring knowledge of integrated absorption. These dimensionless terms are represented by $A_{j \rightarrow j-1}^{0 \rightarrow 1}$ and $A_{j-1 \rightarrow j}^{0 \rightarrow 1}$, respectively, where the superscripts and subscripts denote again the vibrational and rotational transitions, respectively. They have been evaluated at 300, 500, and 1000°K, the results being summarized in Tables VII through IX.

By the combined use of the value of β with the data listed in Tables VII through IX it is possible to evaluate the integrated absorption for the rotational transitions from the relations:

$$S_{j \rightarrow j-1}^{0 \rightarrow 1} = \beta A_{j \rightarrow j-1}^{0 \rightarrow 1} \quad (20)$$

$$S_{j-1 \rightarrow j}^{0 \rightarrow 1} = \beta A_{j-1 \rightarrow j}^{0 \rightarrow 1} \quad (21)$$

Numerical values for $S_{j \rightarrow j-1}^{0 \rightarrow 1}$ and $S_{j-1 \rightarrow j}^{0 \rightarrow 1}$ are also listed in Tables VII to IX.

A revision of integrated absorption values required as the result of a change in effective charge may be accomplished by a recalculation of Tables VII to IX. Relative values of integrated absorption for different rotational transitions are independent of effective charge and may be determined directly from the data available in Tables VII through IX.

The integrated absorption for the rotational lines composing the first overtone will be identified by the symbols $S_{j \rightarrow j-1}^{0 \rightarrow 2}$ and $S_{j-1 \rightarrow j}^{0 \rightarrow 2}$, depending upon the particular rotational transitions which are involved. The quantities $S_{j \rightarrow j-1}^{0 \rightarrow 2}$ and $S_{j-1 \rightarrow j}^{0 \rightarrow 2}$

TABLE VII

TABULATED INTEGRATED ABSORPTIONS FOR CARBON MONOXIDE

AT 300° K

Transition $j \rightarrow j-1$	$10^3 A^0_{j \rightarrow j-1}$	$S^{0+1}_{j \rightarrow j-1}$	Transition $j-1 \rightarrow j$	$10^3 A^0_{j-1 \rightarrow j}$	$S^{0+1}_{j-1 \rightarrow j}$
1 → 0	5.5279	2.0642	0 → 1	5.5716	2.0805
2 → 1	10.712	3.9999	1 → 2	10.879	4.0623
3 → 2	15.279	5.7053	2 → 3	15.641	5.8405
4 → 3	19.016	7.1007	3 → 4	19.619	7.3259
5 → 4	21.735	8.1347	4 → 5	22.647	8.4565
6 → 5	23.514	8.7803	5 → 6	24.639	9.2004
7 → 6	24.236	9.0499	6 → 7	25.579	9.5514
8 → 7	23.996	8.9603	7 → 8	25.535	9.5349
9 → 8	22.969	8.5768	8 → 9	24.634	9.1935
10 → 9	21.317	7.9599	9 → 10	23.038	8.6026
11 → 10	19.227	7.1795	10 → 11	20.940	7.8191
12 → 11	16.834	6.3096	11 → 12	18.529	6.9139
13 → 12	14.453	5.3969	12 → 13	15.985	5.9689
14 → 13	12.074	4.5085	13 → 14	13.456	5.0246
15 → 14	9.8505	3.6782	14 → 15	11.063	4.1310
16 → 15	7.8568	2.9338	15 → 16	8.8886	3.3190
17 → 16	6.1269	2.2878	16 → 17	6.9855	2.6054
18 → 17	4.6734	1.7451	17 → 18	5.3693	2.0051
19 → 18	3.4899	1.3031	18 → 19	4.0391	1.5082
20 → 19	2.5509	.95252	19 → 20	2.9752	1.1110
22 → 21	1.2308	.47826	21 → 22	1.6220	0.60567
24 → 23	0.5924	.22121	23 → 24	0.7725	0.28345
26 → 25	0.2529	.094435	25 → 26	0.3399	0.12692
28 → 27	0.0998	.037266	27 → 28	0.1383	.051642
30 → 29	0.0364	.013592	29 → 30	0.0521	.019455
35 → 34	0.0021	.0078415	34 → 35	0.0014	.0052276
40 → 39	0.0001	.00373407	39 → 40	0.0000	0.00000

TABLE VIII

TABULATED INTEGRATED ABSORPTIONS FOR CARBON MONOXIDE

AT 500° K

Transition

Transition

$j \rightarrow j$	$10^2 A^0 j \rightarrow j-1$	$S_{j-1 \rightarrow j}^{0 \rightarrow 1}$	$j \rightarrow j-1$	$10^2 A^0 j-1 \rightarrow j$	$S_{j \rightarrow j-1}^{0 \rightarrow 1}$
0 → 1	4.4239	0.76902	1 → 0	4.4215	0.76861
1 → 2	8.702	1.51270	2 → 1	8.6955	1.51157
2 → 3	12.698	2.20734	3 → 2	12.681	2.20439
3 → 4	16.286	2.83106	4 → 3	16.250	2.82400
4 → 5	19.356	3.36473	5 → 4	19.325	3.35934
5 → 6	21.863	3.80053	6 → 5	21.829	3.79462
6 → 7	23.753	4.12908	7 → 6	23.671	4.11482
7 → 8	24.949	4.33698	8 → 7	24.861	4.32169
8 → 9	25.532	4.43833	9 → 8	25.437	4.42181
9 → 10	25.525	4.43711	10 → 9	25.425	4.41973
11 → 12	24.049	4.18053	12 → 11	23.869	4.14924
13 → 14	21.076	3.66372	14 → 13	20.343	3.62322
15 → 16	17.316	3.01011	16 → 15	17.054	2.96457
17 → 18	13.401	2.32955	18 → 17	13.139	2.28400
19 → 20	9.8041	1.70429	20 → 19	9.5657	1.66234
21 → 22	6.7962	1.18141	22 → 21	6.5965	1.14670
23 → 24	4.4719	0.77737	24 → 23	4.3162	0.75030
25 → 26	2.7993	0.48661	26 → 25	2.6840	0.46657
27 → 28	1.6649	0.28942	28 → 27	1.5877	0.27600
29 → 30	9.4388×10^{-1}	0.16408	30 → 29	.89436	0.15547
31 → 32	5.1001×10^{-1}	0.088658	32 → 31	.48009	0.083456
33 → 34	2.6287×10^{-1}	0.045696	34 → 33	.24575	0.042720
35 → 36	1.2923×10^{-1}	0.022473	36 → 35	.12002	0.020364
37 → 38	6.0739×10^{-2}	0.010559	38 → 37	.56013 $^{-1}$.009737
39 → 40	2.7258×10^{-2}	0.0047384	40 → 39	.24910 $^{-1}$.004330
41 → 42	1.1678×10^{-2}	0.0020300	42 → 41	.10598 $^{-1}$.001842
43 → 44	4.7830×10^{-3}	0.00083195	44 → 43	.43000 $^{-2}$.000749
45 → 46	1.8720×10^{-3}	.00032542	46 → 45	.16746 $^{-2}$.0002911
47 → 48	7.0211×10^{-4}	.00012205	48 → 47	.62247 $^{-3}$.0001032
49 → 50	2.5196×10^{-4}	.000043799	50 → 49	.22144 $^{-3}$.00003849
51 → 52	8.5011×10^{-5}	.000014778	52 → 51	.75306 $^{-4}$.00001309
53 → 54	2.7874×10^{-5}	.0000048455	54 → 53	.24546 $^{-4}$.000004267
55 → 56	6.8517×10^{-6}	.0000011911	56 → 55	.7242 $^{-5}$.000001343

TABLE IX

 TABULATED INTEGRATED ABSORPTIONS FOR CARBON MONOXIDE
 AT 1000° K

Transition j→j-1	$10^2 A^0_{j\rightarrow j-1}$	10 S $0\rightarrow 1$ $j\rightarrow j-1$	Transition j-1→j	$10^2 A^0_{j-1\rightarrow j}$	10 S $0\rightarrow 1$ $j-1\rightarrow j$
1 → 0	20.134	1.80576	0 → 1	20.039	1.79724
2 → 1	40.023	3.53955	1 → 2	39.654	3.55646
4 → 3	77.763	6.97435	3 → 4	76.330	6.84583
6 → 5	110.80	9.93735	5 → 6	107.76	9.66470
8 → 7	137.25	12.30958	7 → 8	132.24	11.86025
10 → 9	155.86	13.97866	9 → 10	148.78	13.34366
12 → 11	166.17	14.90333	11 → 12	157.12	14.09167
14 → 13	168.43	15.10603	13 → 14	157.77	14.14997
16 → 15	163.55	14.66835	15 → 16	151.76	13.61094
18 → 17	152.90	13.71319	17 → 18	140.53	12.60376
20 → 19	138.06	12.38223	19 → 20	125.23	11.23154
22 → 21	120.74	10.82854	21 → 22	108.83	9.76067
24 → 23	102.39	9.18308	23 → 24	91.406	8.19796
26 → 25	84.367	7.56665	25 → 26	74.564	6.68744
28 → 27	67.591	6.06205	27 → 28	59.140	5.30411
30 → 29	52.699	4.72643	29 → 30	45.649	4.09414
32 → 31	40.024	3.58964	31 → 32	34.310	3.07717
34 → 33	29.621	2.65662	33 → 34	22.865	2.05070
36 → 35	21.370	1.91662	35 → 36	17.941	1.60908
38 → 37	15.044	1.34926	37 → 38	12.494	1.12055
40 → 39	10.332	0.92656	39 → 40	8.4898	0.76143
42 → 41	6.9282	0.62137	41 → 42	5.6292	0.50437
44 → 43	4.5350	0.406732	43 → 44	3.6443	0.32685
46 → 45	2.8999	0.26008	45 → 46	2.3033	0.20658
48 → 47	1.8112	0.16244	47 → 48	1.4222	0.12755
50 → 49	1.1058	0.099176	49 → 50	0.8581	0.07696
52 → 51	0.6598	0.059176	51 → 52	0.5058	0.04536
54 → 53	0.3848	0.034511	53 → 54	0.2915	0.02614
56 → 55	0.2213	0.019848	55 → 56	0.1712	0.01535
58 → 57	0.1225	0.010936	57 → 58	0.0771	0.006915
60 → 59	0.0668	0.005991	59 → 60	0.0485	0.004350
62 → 61	0.0357	0.003203	61 → 62	0.0270	0.002422
64 → 63	0.0186	0.001668	63 → 64	0.0139	0.001247
66 → 65	0.0095	0.000852	65 → 66	0.0071	0.000636
68 → 67	0.0048	0.000430	67 → 68	0.0035	0.000313
70 → 69	0.0023	0.000206	69 → 70	0.0017	0.000152
72 → 71	0.0011	0.000098	71 → 72	0.0008	0.000071
74 → 73	0.0005	0.000044	73 → 74	0.0004	0.0000353

TABLE X

TABULATED INTEGRATED ABSORPTIONS FOR CARBON MONOXIDE AT 300°

Transition $j \rightarrow j - 1$	$10^2 S \frac{0}{j} \rightarrow \frac{2}{j-1}$	Transition $j - 1 \rightarrow j$	$10^2 S \frac{0}{j-1} \rightarrow \frac{2}{j}$
1 → 0	1.42343	0 → 1	1.43971
2 → 1	2.76793	1 → 2	2.81111
3 → 2	3.94307	2 → 3	4.04163
4 → 3	4.91368	3 → 4	5.06952
5 → 4	5.62921	4 → 5	5.85190
6 → 5	6.07597	5 → 6	6.36668
7 → 6	6.26253	6 → 7	6.60957
8 → 7	6.20053	7 → 8	6.59815
9 → 8	5.93510	8 → 9	6.36536
10 → 9	5.50325	9 → 10	5.95300
11 → 10	4.96821	10 → 11	5.41062
12 → 11	4.36624	11 → 12	4.73766
13 → 12	3.73465	12 → 13	4.13048
14 → 13	3.11936	13 → 14	3.47702
15 → 14	2.54531	14 → 15	2.85865
16 → 15	2.03019	15 → 16	2.29675
17 → 16	1.58316	16 → 17	1.80501
18 → 17	1.20761	17 → 18	1.38753
19 → 18	0.901705	18 → 19	1.04367
20 → 19	0.659144	19 → 20	0.768812
22 → 21	0.330956	21 → 22	0.419124
24 → 23	0.153077	23 → 24	0.199607
26 → 25	.065349	25 → 26	.037526
23 → 27	.025753	27 → 28	.035736
30 → 29	.009405	29 → 30	.013463
35 → 34	.005426	34 → 35	.0036175
40 → 39	.002840	39 → 40	.00000



are obtained from $S_{j \rightarrow j-1}^{0 \rightarrow 1}$ and $S_{j-1 \rightarrow j}^{0 \rightarrow 1}$, respectively, by multiplying by the ratio of integrated absorption of the first overtone to the integrated absorption for the fundamental. The experimentally observed ratio⁽¹⁷⁾ is

$$1.64/237 = 6.92 \times 10^{-3} \quad (22)$$

Using this ratio, the results summarized in Table X are obtained for $S_{j \rightarrow j-1}^{0 \rightarrow 2}$ and $S_{j-1 \rightarrow j}^{0 \rightarrow 2}$ at 300°K.

D. Methods for the Determination of the Complete Partition Function

The complete partition function

$$Q_{vjm} = \sum_n \sum_j (2j+1) \exp - (E_n, j/kT)$$

may be evaluated by standard statistical methods.⁽¹⁰⁾

If the molecule is approximated as an ideal diatomic gas, i.e., a diatomic gas whose energy is equal to the sum of the energies of a one-dimensional harmonic oscillator and of a rigid rotator, then it can be shown that⁽¹⁰⁾

$$Q_{vjm} = \frac{1}{\sigma(1-e^{-u})} \left(1 + \frac{\sigma}{3} + \frac{\sigma^2}{15} + \frac{4\sigma^3}{315} + \dots \right) e^{-u\sigma} \quad (23)$$

where

T = absolute temperature (°K)

h = Planck's constant = $(6.6242 \times 10^{-27}$ erg-sec)

k = the Boltzmann constant = 1.38048×10^{-16} erg/°K

ν = the vibrational frequency of the molecule under consideration

σ_T = $h^2/3\pi^2 lk$

uT = $h\nu/k$

The spectroscopic data for carbon monoxide collected by Sponer⁽¹¹⁾ lead to the results

$$\sigma T = 2.743 \text{ degrees}$$

$$uT = 3066.9 \text{ degrees.}$$

Using these data, representative numerical values of Q_{vjm} for carbon monoxide treated as an ideal diatomic gas are summarized below:

TABLE XI

Q_{vjm} FOR CO (ASSUMED AN IDEAL DIATOMIC GAS) AS A FUNCTION OF T

T(K)	Q_{vjm}
300	0.66122
500	8.52205
1000	82.5871

If allowance is made for vibration-rotation interactions within the molecules, and using an expression for the internal energy of the form given in Eq. (23), it is found that the partition function for the general diatomic gas⁽¹⁰⁾ is

$$Q_{vjm} = \frac{1}{\sigma(1-e^{-u})} \left[1 + \frac{\sigma}{3} + \frac{8\gamma^2}{\sigma} + \frac{\delta}{(e^{u-1})} + \frac{2\chi u}{(e^{u-1})^2} \right] \left[\exp - \left(\frac{u}{2} \left[\frac{1}{1-2\chi e} - \frac{\chi^2}{2} \right] \right) \right] \quad (24)$$

where $\exp - \left(\frac{u}{2} \left[\frac{1}{1-2\chi e} - \frac{\chi^2}{2} \right] \right)$

is derived from $\exp - (E_{o,0}/kT)$

and

T = absolute temperature ($^{\circ}\text{K}$)

c = velocity of light = 2.9977×10^{10} cm/sec

\bar{T} = $\text{Bohr}/k = 2.743$ degrees

\bar{w} = $hc\kappa_0(1 - x_0)/k = 3066.9$

γ = 0.00394

δ = 0.0091

B_0 = 1.916 cm^{-1}

Numerical values of Q_{vjm} calculated using Eq. (24) are summarized below:

TABLE XIII

Q_{vjm} FOR CO (GENERAL DIATOMIC GAS, VIBRATION ROTATION INTERACTION) AS A
FUNCTION OF T

<u>T($^{\circ}\text{K}$)</u>	<u>Q_{vjm}</u>
300	0.630956
500	8.292231
1000	81.650755

IV. EMISSIVITY CALCULATIONS FOR DIATOMIC GASES WITH NON-OVERLAPPING ROTATIONAL LINES

The basic equation for making emissivity calculations has been given previously in Eq. (11), viz.,

$$\epsilon = \int_{-\infty}^{\infty} J_{\nu} d\nu / \sigma T^4 \quad (11)$$

If J_{ν} is calculated from Eq. (8) and P_{ν} is determined from the dispersion formula presented in Eq. (7), then Eq. (11) can be used for calculating the emissivity at all values of the total pressure and the optical density. A calculation of this sort is extremely laborious and requires numerical integrations. For this reason the present discussion will be restricted to developing appropriate relations for calculating the emissivity for non-overlapping rotational lines. The results of these calculations will supplement previously published data which are reliable only under conditions of extensive overlapping of rotational lines. (5,7)

At low pressures the rotational lines are so narrow that the contribution to P_{ν} at any wave number will originate with but a single rotational line. This means, for example, that in the vicinity of the rotational line whose center is at $\nu^{0 \rightarrow 1}_{j \rightarrow j-1}$, the only term which makes an appreciable contribution in the evaluation of P_{ν} in that region is

$$\frac{S_{j \rightarrow j-1}^{0 \rightarrow 1}}{((\nu - \nu_{j \rightarrow j-1}^{0 \rightarrow 1})^2 + \alpha^2)}$$

Therefore, it is possible to subdivide the interval of integration of

Eq. (7) in such a manner that each subinterval is centered about one of the wave numbers $\nu_j^0 \rightarrow \frac{1}{j \rightarrow j \pm 1}$. Within the limits of error of the assumption of non-overlapping lines, the following close approximation is obtained:

$$\int_{-\infty}^{\infty} J_r dr = \sum_{\Delta r_i} \left\{ J^0(\nu_{j \rightarrow j-1}^0) \int_{\Delta r_i} [1 - e^{-(P_{j \rightarrow j-1}^0, PL)}] dr + J^0(\nu_{j-1 \rightarrow j}^0) \int_{\Delta r_i} [1 - e^{-(P_{j-1 \rightarrow j}^0, PL)}] dr \right\} \quad (25)$$

Here $J^0(\nu_j^0 \rightarrow \frac{1}{j \rightarrow j-1})$ and $J^0(\nu_{j-1 \rightarrow j}^0)$ represent, to a very close approximation, the spectral intensities of a blackbody radiator evaluated at the line centers corresponding to the indicated transitions.

Similarly, $P_{j \rightarrow j-1}^0$ and $P_{j-1 \rightarrow j}^0$ are the characteristic values of the spectral absorption coefficient which would be valid if only the indicated transitions occurred. The actual extent of the subintervals Δr_i may be chosen arbitrarily. For convenience, they may be chosen to extend from a wave number midway between two line centers to the wave number midway between the next successive line centers. The subintervals need not be of equal width. The error introduced by replacing

$$\int_{\Delta r_i} [1 - e^{-(P_{j \rightarrow j-1}^0, PL)}] dr$$

by

$$\int_{-\infty}^{\infty} [1 - e^{-(P_{j \rightarrow j-1}^0, PL)}] dr$$

for the non-overlapping condition is negligibly small at low values of optical density. The magnitude of this error increases with increasing optical density PL , i.e., increased overlapping of rotational lines, and

can be estimated readily by numerical calculations of the type described in Section V.A. The summation indicated by Eq. (25) then becomes

$$\int_{-\infty}^{\infty} J_r dr = \sum_j \left\{ J^o(\nu_{j-j-1}^{o+1}) \int_{-\infty}^{\infty} [1 - e^{-(P_{j-j-1}^{o+1}, PL)}] dr + J^o(\nu_{j-1-j}^{o+1}) \int_{-\infty}^{\infty} [1 - e^{-(P_{j-1-j}^{o+1}, PL)}] dr \right\} \quad (26)$$

Infinite integrals of this type have been evaluated by Ladenburg and Reiche for spectral absorption coefficients given by Eq. (6). The integrations result in the expression

$$\int_{-\infty}^{\infty} [1 - e^{-(P_{j-j \pm 1}^{n-n+1}, PL)}] dr = 2\pi\alpha \kappa_j e^{-\kappa_j} [J_0(i\kappa_j) - iJ_1(i\kappa_j)] \quad (27)$$

where

$$\kappa_j = S \frac{n \rightarrow n+1}{j \rightarrow j \pm 1} PL / 2\pi\alpha$$

J_0 = Bessel function of zero order

J_1 = Bessel function of first order.

Substitution into Eq. (26) results in

$$\begin{aligned} \int_{-\infty}^{\infty} J_r dr &= 2\pi\alpha \sum_j \left\{ J^o(\nu_{j-j-1}^{o+1}) \kappa_j e^{-\kappa_j} [J_0(i\kappa_j) - iJ_1(i\kappa_j)] \right. \\ &\quad \left. + J^o(\nu_{j-1-j}^{o+1}) \kappa_{j-1} e^{-\kappa_{j-1}} [J_0(i\kappa_{j-1}) - iJ_1(i\kappa_{j-1})] \right\} \end{aligned} \quad (28)$$



where

$$\chi_j = S \begin{smallmatrix} 0 \\ j \rightarrow 1 \end{smallmatrix} pL/2\pi\alpha$$

$$\chi_{j-1} = S \begin{smallmatrix} 0 \\ j-1 \rightarrow j \end{smallmatrix} pL/2\pi\alpha$$

This equation indicates the method of calculation of the summed intensity of radiation of a series of non-overlapping rotational lines composing a given vibration-rotation band.

Eq. (27) may be used to obtain asymptotic limiting forms for small and large values of χ_j . The Bessel function $J_n(x)$ can be written⁽¹⁸⁾ as a power series in $x/2$ as follows:

$$J_n(x) = \frac{(x/2)^n}{0! n!} - \frac{(x/2)^{n+2}}{1! (n+1)!} + \frac{(x/2)^{n+4}}{2! (n+2)!} - \frac{(x/2)^{n+6}}{3! (n+3)!} + \dots$$

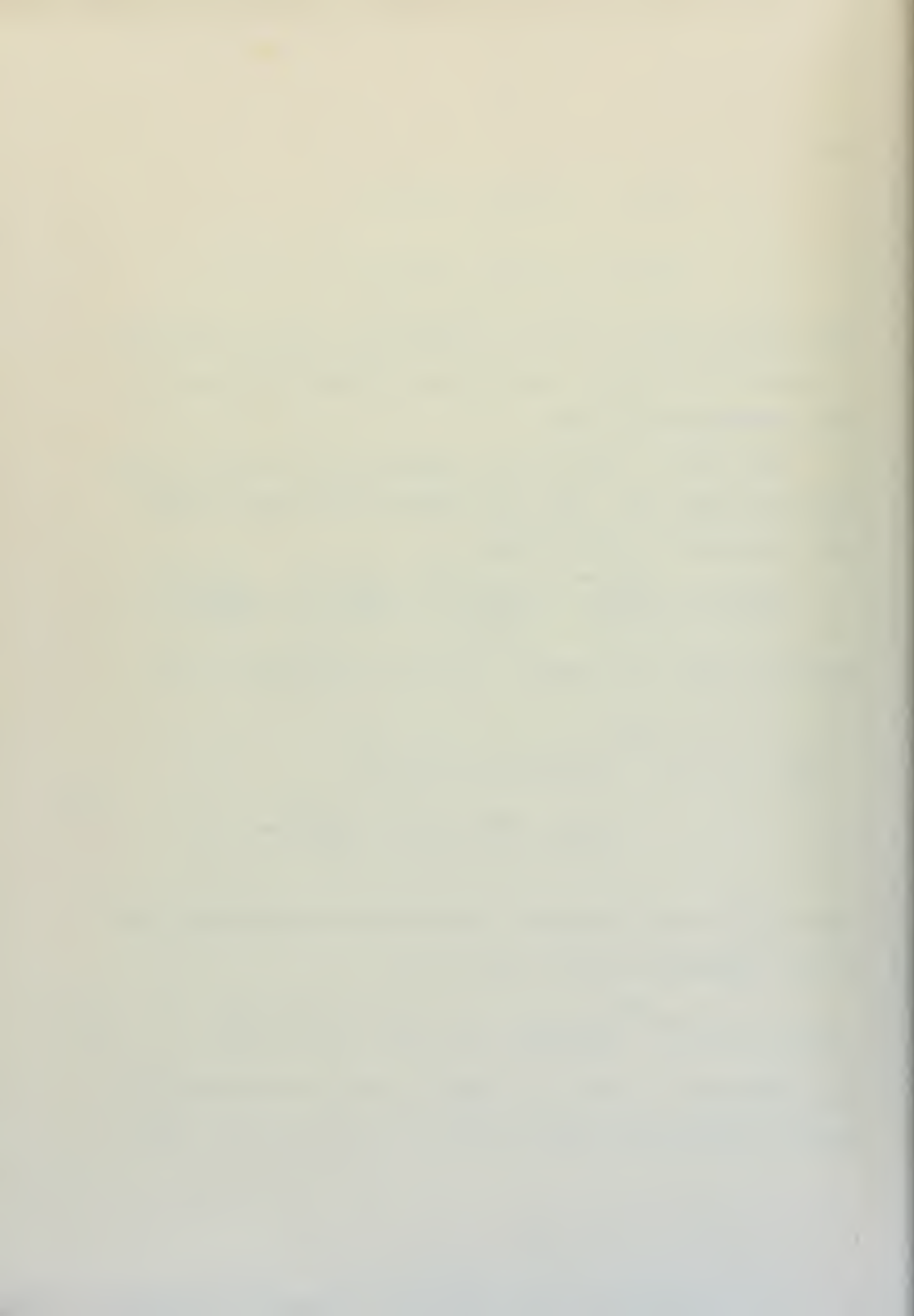
Therefore, incorporating suitable expansions of the remaining terms,

$$\lim_{\chi_j \rightarrow 0} \chi_j e^{-\chi_j} [J_0(i\chi_j) - i J_1(i\chi_j)] = \chi_j (1 - \frac{\chi_j}{2} + \frac{\chi_j^2}{4} - \frac{5\chi_j^3}{48} + \dots) \quad (29)$$

where only the first term need be retained for sufficiently small values of χ_j . Similarly, for large values of χ_j ,

$$\lim_{\chi_j \rightarrow \infty} 2\pi\alpha \chi_j e^{-\chi_j} [J_0(i\chi_j) - i J_1(i\chi_j)] = 2\alpha \sqrt{2\pi\chi_j} \quad (30)$$

The application of Eq. (29) is particularly useful in calculations involving non-overlapping rotational lines. The condition of large χ_j ,



for which Eq. (30) applies, generally implies the occurrence of a appreciable overlapping between rotational lines.

At elevated temperatures it is necessary to consider the contributions from vibrational transitions other than the $0 \rightarrow 1$ transitions. For this reason, the total radiation intensity must be calculated by including in the sum indicated in Eq. (28) terms resulting from the higher vibrational transitions ($2 \rightarrow 1$, $3 \rightarrow 2$, $4 \rightarrow 3$, etc., in addition to $1 \rightarrow 0$). Furthermore, at large optical densities, overtone transitions may make appreciable contributions such that the vibrational transitions $2 \rightarrow 0$, $3 \rightarrow 1$, $4 \rightarrow 2$, etc. must be considered.

For non-overlapping rotational lines the intensity of radiation emitted by the first overtone is given by an obvious modification of Eq. (28). Thus, for the first overtone of CO,

$$\int_{-\infty}^{\infty} J_{\nu} d\nu = 2\pi\alpha \sum_j \left\{ J^o(\nu_{j+j-1}^{o+2}) \chi'_j e^{-\chi'_j [J_0(i\chi'_j) - iJ_1(i\chi'_j)]} + J^o(\nu_{j-1+j}^{o+2}) \chi'_{j-1} e^{-\chi'_{j-1} [J_0(i\chi'_{j-1}) - iJ_1(i\chi'_{j-1})]} \right\} \quad (31)$$

where

$$\chi'_j = S_{j \rightarrow j-1}^{0 \rightarrow 2} pL/2\pi\alpha$$

$$\chi'_{j-1} = S_{j-1 \rightarrow j}^{0 \rightarrow 2} pL/2\pi\alpha .$$

V. NUMERICAL EMISSIVITY CALCULATIONS FOR CARBON MONOXIDE AT 300° K

This section will be devoted to the numerical emissivity calculations of carbon monoxide at 300° K.

A. Overlapping Between Adjacent Rotational Lines

As was discussed in Sections III and IV, emissivity calculations for non-overlapping lines, at temperatures low enough to permit neglect of Doppler broadening, can be carried out since the rotational line-shape is represented satisfactorily by the dispersion formula of Lorentz, Eq. (6).

To illustrate the effect of overlapping on P_{ν} , representative calculations involving the contributions to P_{ν} from two adjacent rotational lines have been carried out. In this case the correct expression for the emissivity is evidently

$$E_{\nu} = 1 - \exp \left[- (P_{\nu_1} + P_{\nu_2}) pL \right] \quad (32)$$

where P_{ν_1} and P_{ν_2} represent, respectively, the values of the spectral absorption coefficients arising from each of the two rotational lines separately. If the two rotational lines are separated sufficiently to permit neglect of overlapping, then the spectral emissivity is represented by the relation

$$E'_{\nu} = 1 - \exp (-P_{\nu_1} pL) + 1 - \exp (-P_{\nu_2} pL) \quad (33)$$

By evaluating the difference $E_{\nu} - E'_{\nu}$ from Eqs. (32) and (33) we can determine the error incurred in making numerical emissivity calculations

if overlapping between two adjacent rotational lines is ignored. The resulting expression is

$$\mathcal{E}_\nu - \mathcal{E}'_\nu = -(P_{\nu_1} \times P_{\nu_2}) p^2 L^2 + \frac{(P_{\nu_1}^2 P_{\nu_2} + P_{\nu_1} P_{\nu_2}^2) p^3 L^3}{2} + \dots \quad (34)$$

which can be used to estimate the amount by which neglect of overlapping between adjacent lines overestimates the value of the emissivity for small values of P_{ν_1} , pL and P_{ν_2} , pL .

Emissivity calculations for two rotational lines based on the correct expression given in Eq. (32), can be used as a qualitative guide in ascertaining the limits of validity of theoretical calculations based on a treatment for non-overlapping rotational lines. Thus if the optical density is sufficiently small to permit neglect of overlapping between the two strongest adjacent rotational lines, then emissivity calculations based on Eq. (28) should give valid results.

In Fig. 1 the spectral absorption coefficient P_ν is shown as a function of ν at a total pressure of 1 atm, as calculated from Eq. (7). The rotational half-width used to construct Fig. 1 is $\alpha = 0.06 \text{ cm}^{-1}$. Reference to Fig. 1 shows that the spectral absorption coefficient is a rapidly varying function of ν at small total pressures.

Representative values of \mathcal{E}_ν calculated from Eq. (32) are shown in Figs. 2 and 3 as a function of ν with pL treated as a variable parameter. Reference to Fig. 2 indicates that the emissivity at a point midway between the rotational line centers which are characterized by the transitions $n = 0 \rightarrow n = 1$, $j = 8 \rightarrow j = 7$ and $j = 7 \rightarrow j = 6$, respectively, remains very small (i.e., $\mathcal{E}_\nu < 0.2$) for $pL \leq 2 \text{ cm} - \text{atm}$. Since the

indicated transitions correspond to the two most intense rotational lines (compare Table VII) it appears justifiable to conclude that emissivity calculations based on the use of Eq. (23) will yield valid results for $pL \leq 2 \text{ cm} - \text{atm}$. Calculations similar to those shown in Fig. 2 for intense adjacent rotational lines are shown in Fig. 3 for weak rotational lines, namely, for the lines corresponding to the transitions $n = 0 \rightarrow n = 1$, $j = 19 \rightarrow j = 18$, and $j = 18 \rightarrow j = 17$. As is to be expected, the emissivity ϵ_ν is represented more adequately by Eq. (33) for larger values of pL than it was for the more intense rotational lines described in Fig. 2. Although the precise evaluation of errors arising from the use of Eq. (23) is difficult to carry out, it is evident from the data described in Figs. 2 and 3 that the calculated values of the emissivity are reliable at least to $pL = 2 \text{ cm} - \text{atm}$ and probably to somewhat larger values. This conclusion is borne out by the comparison between calculated and observed emissivities described in Section V.B.

B. Description of Emissivity Calculations for CO Assuming No Overlapping Between Rotational Lines

This section will be devoted to the detailed description of the application of the mathematical formulations outlined in Section IV for the calculation of the emissivity of carbon monoxide in the special case when overlapping between rotational lines can be neglected. A detailed calculation will be described for the following special conditions:

Temperature = 300°K

Critical density = $0.1 \text{ cm}^{-3} \text{ atm}$

Rotational half-width = 0.003 cm^{-1} at atmospheric pressure

The sample calculation will be carried out by determining first the contributions to the intensity of radiation made by two rotational lines, then to perform the summation over the contributions made by all rotational lines, and finally to convert the summed radiant intensity to emissivity.

The working equation from which values of the intensity of radiation from a single rotational transition in the fundamental vibration-rotation band can be obtained is derived from Eq. (20) and can be expressed as

$$I_j = J^0(\nu_{j \rightarrow j+1}^0) \kappa_j e^{-\kappa_j} [J_0(i\kappa_j) - i J_1(i\kappa_j)] \quad (35)$$

where

I_j = intensity of radiation from a single rotational line,

J^0 = blackbody intensity of radiation evaluated at the line center for the indicated transition,

$$\kappa_j = S \sum_{j \rightarrow j+1}^{0 \rightarrow 1} \frac{pL}{2\pi c} .$$

The best available experimental data indicate that the value of the rotational half-width α at 300°K is 0.077 cm^{-1} .⁽¹⁷⁾ However, the value used in this sample calculation will be 0.003 cm^{-1} , the error introduced being of the order of 3% since the emissivity for non-overlapping lines is roughly proportional to the assumed rotational half-width (see Section V.C).

Numerical values of the integrated absorption of rotational lines at 300°K have been summarized in Table VII. If the value of the integrated absorption for any given transition is known, then the term χ_j can be evaluated for any optical density.*

Representative numerical values are listed in the following Table XIII.

TABLE XIII

CALCULATION OF THE TERM χ_j FOR TWO
GIVEN TRANSITIONS

Transition	$S^0 \rightarrow 1$ $j \rightarrow j \pm 1$	pL	α	$\chi_j = S^0 \rightarrow 1$ $j \rightarrow j \pm 1$ pL/2πα
$1 \rightarrow 0$	$2.0642 \text{ atm}^{-1} \text{ cm}^{-2}$	0.1 cm atm	0.08 cm^{-1}	0.521475
$10 \rightarrow 9$	$7.9599 \text{ atm}^{-1} \text{ cm}^{-2}$	0.1 cm atm	0.08 cm^{-1}	1.58354

The term χ_j is evidently dimensionless. The terms $e^{-\chi_j}$, $J_0(i\chi_j)$ and $-iJ_1(i\chi_j)$ are determined from compilations such as those given by Jahnke and Emde⁽²⁰⁾. Thus the quantity,

$$F(\chi_j) = 2\pi\alpha \chi_j e^{-\chi_j} [J_0(i\chi_j) - iJ_1(i\chi_j)]$$

may be calculated.

* Reference to Tables XVI(a and b) and XVII(a and b) throughout this discussion will clarify the entire procedure used for numerical calculations.

Results of this calculation for the rotational transitions $1 \rightarrow 0$ and $10 \rightarrow 9$ are given in the following Table XIV.

TABLE XIV

CALCULATION OF THE TERM $F(\chi_j)$ FOR TWO GIVEN TRANSITIONS

TRANSITION	χ_j	$e^{-\chi_j}$	$J_0(i\chi_j)$	$-2J_1(i\chi_j)$	$J_0 - iJ_1$	$F(\chi_j)$
$1 \rightarrow 0$	0.521475	0.59364	1.06920	0.269711	1.33891	0.20539 cm^{-1}
$10 \rightarrow 9$	1.58354	.20525	1.73229	1.06725	2.79954	0.45739 cm^{-1}

The desired units for the intensity of radiation are ergs $\text{cm}^{-2}\text{sec}^{-1}$. Since the units of the term $F(\chi_j)$ are cm^{-1} , it is obvious that the term $J^0(\nu_{j \rightarrow j+1})$ must be expressed in ergs $\text{cm}^{-1} \text{ sec}^{-1}$. Tables of Radiation Functions⁽¹⁹⁾ list the ratio $R_\lambda / R_{\lambda \text{ max}}$ as a function of $\lambda T (\text{cm}^{-0}\text{K})$.

The term $R_\lambda / R_{\lambda \text{ max}}$ is equal to the energy emitted by a blackbody at the absolute temperature T per unit time, per unit area, in a wave length interval between λ and $\lambda + d\lambda$, throughout the solid angle 2π steradians, divided by the maximum value of R_λ which is designated as $R_{\lambda \text{ max}}$. The quantity $R_{\lambda \text{ max}}$ is given by the expression,

$$R_{\lambda \text{ max}} = 21.20144 c_1 (T/c_2)^5 \text{ erg cm}^{-3} \text{ sec}^{-1} \quad (36)$$

where

$$c_1 = 3.732 \times 10^{-5} \text{ erg cm}^2 \text{ sec}^{-1}$$

$$c_2 = 1.436 \text{ cm}^{-0}\text{K}$$

At 300°K it is found from Eq. (36) that

$$R_{\lambda \max} = 3.1488 \times 10^8 \text{ ergs cm}^3 \text{ sec}^{-1}$$

Using this value for $R_{\lambda \max}$, it is a simple matter to calculate R_{λ} and R_{λ} / ν^2 , which has the desired dimensions of $\text{ergs cm}^{-1} \text{ sec}^{-1}$. The product of R_{λ} / ν^2 and $F(X_j)$ represents the total radiant intensity contributed by a given rotational line. The various intermediate steps involved in the calculation of I_j are listed in Table XV for two representative rotational lines.

For any specified conditions, the total intensity of radiation can be found by summing the contributions made by the rotational lines composing a given vibration-rotation band according to Eq. (28). Detailed calculations at atmospheric pressure and 300°K for an optical density of 0.1 cm-atm are shown in Tables XVI(a and b) and XVII(a and b).

Reference to either Eq. (5) or Eq. (11) indicates that the value of emissivity is obtained from the value of total intensity of radiation by a division by the value of the total blackbody intensity of radiation under the given conditions. This quantity is designated by $R_{o \rightarrow \infty}$ in tables of Planck's Radiation Functions and is conveniently calculated from Eq. (10) or the equivalent relation:

$$R_{o \rightarrow \infty} \equiv 6.493939 c_1 (T/c_2)^4 \quad (37)$$

At 300°K it is found that $R_{o \rightarrow \infty} = 4.61655 \times 10^5 \text{ erg cm}^{-2} \text{ sec}^{-1}$. This value of $R_{o \rightarrow \infty}$ has been used for the calculation of the emissivity listed in Tables XVI(a and b).

TABLE XV

INTERMEDIATE STEPS FOR THE CALCULATION OF RADIANT INTENSITY FOR TWO GIVEN TRANSITIONS

Transi-tion	Line Center ν (cm^{-1})	$\lambda \tau$	$R_A / R_{A,\text{max}}$	R_A	μ^2	R_A / μ^2	$F(\chi_i)$	I_j
$1 \rightarrow 0$	2138.4	4.676×10^3	.14029	.190127	5.9367×10^7	4.5726×10^6	13.0920	0.61333 2.7273
$10 \rightarrow 9$	2102.1	4.7571×10^3	.14272	.20792	6.5463×10^7	4.4133×10^6	14.3153	.45739 6.7765

TABLE XVI(a)

WORK SHEET FOR THE CALCULATION OF THE EMISSIVITY OF CARBON

MONOXIDE AT 300°K ($\alpha = 0.08 \text{ cm}^{-1}$, $pL = 0.1$) ($j \rightarrow j \pm 1$)

Transition $j \rightarrow j - 1$	$S_{j \rightarrow j-1}^{o \rightarrow '}$	χ_j	$e^{-\chi_j}$	$J_o(i\chi_j)$	$-iJ_1(i\chi_j)$
1 → 0	2.0642	.521475	.59364	1.06920	0.269711
2 → 1	3.9999	1.04867	.35040	1.29440	.599829
3 → 2	5.7053	1.44132	.23661	1.59063	.924754
4 → 3	7.1007	1.79384	.16632	1.98138	1.30944
5 → 4	8.1347	2.05505	.12009	2.36958	1.67428
6 → 5	8.7803	2.21815	.10381	2.66430	1.94667
7 → 6	9.0499	2.28626	.10165	2.80115	2.07109
8 → 7	89603	1.78256	.16821	1.96633	1.29537
9 → 8	8.5768	1.70627	.18154	1.87152	1.20364
10 → 9	7.9599	1.56354	.20525	1.73229	1.06725
11 → 10	7.1795	1.42829	.23972	1.57824	.912393
12 → 11	6.3096	1.25523	.28501	1.43447	.759641
13 → 12	5.3969	1.07366	.34176	1.30967	.570008
14 → 13	4.5085	.39692	.40782	1.21146	.495067
15 → 14	3.6782	.73174	.48107	1.13840	.390944
16 → 15	2.9336	.58365	.55786	1.03700	.304844
17 → 16	2.2878	.45513	.63436	1.005248	.233470
18 → 17	1.7451	.34717	.79559	1.03039	.176228
19 → 18	1.3031	.25924	.77164	1.01690	.130712
20 → 19	0.95252	.18949	.82738	1.00895	.0951450
22 → 21	0.47326	.095145	.90924	1.00226	.0476240
24 → 23	0.22121	.044008	.95694	1.00048	.0220040
26 → 25	0.094435	.018787	.93138	1.00009	.0093935
28 → 27	0.037266	.0074137	.99261	1.0000	.0037065
30 → 29	0.013592	.0027040	.99730	1.0000	.0013520
40 → 39	.0037341	.00074206	.99926	1.0000	.0003714

TABLE XVI(a) (CONTINUED)

Transition $j \rightarrow j - 1$	$J_0(i\chi_j)$ $-iJ_1(i\chi_j)$	$F(\chi_j)$	$\frac{J_\nu(300)}{\nu^2}$	I_j
1 → 0	1.33891	.208349	13.0920	2.72777
2 → 1	1.39423	.349880	13.2654	4.64130
3 → 2	2.51538	.431201	13.4525	5.80073
4 → 3	3.25082	.437533	13.6361	6.64805
5 → 4	4.04366	.535078	13.8260	7.39799
6 → 5	4.61097	.559416	14.0122	7.83865
7 → 6	4.87304	.569267	14.2110	8.08985
8 → 7	3.26170	.491613	14.4075	7.08291
9 → 8	3.07516	.478818	14.6183	6.99951
10 → 9	2.79954	.457385	14.8158	6.77652
11 → 10	2.49123	.428763	15.0252	6.44225
12 → 11	2.19411	.394571	15.2813	6.02956
13 → 12	1.32768	.337110	15.4604	5.21136
14 → 13	1.79653	.313776	15.6620	4.92064
15 → 14	1.52934	.270615	15.9053	4.30421
16 → 15	1.39184	.227798	16.1368	3.67593
17 → 16	1.28595	.186629	16.3791	3.05514
18 → 17	1.20662	.143307	16.6164	2.47264
19 → 18	1.14761	.115397	16.8664	1.94633
20 → 19	1.10410	.0870127	17.1304	1.49056
22 → 21	1.04908	.0456549	17.6633	.806416
24 → 23	1.02248	.0216448	18.2139	.394236
26 → 25	1.00948	.0093568	18.7973	.175862
28 → 27	1.00371	.00371283	19.3927	.0720018
30 → 29	1.00135	.00135738	20.0097	.0271608
40 → 39	1.00037	.000373275	23.5833	.0088036

$$\sum I_j = 107.249$$

$$E_i = \frac{\sum I_j}{R_{o \rightarrow \infty}} = \frac{107.249}{4.6166 \times 10^5} = 2.32314 \times 10^{-4}$$

TABLE XVI(b)

WORK SHEET FOR THE CALCULATION OF THE KISSLIVITY OF CARBON
MONOXIDE AT 300°K ($\alpha = 0.03 \text{ cm}^{-1}$, $pL = 0.1$) ($j \rightarrow j + 1$)

Transition $j - 1 \rightarrow j$	$S_{j-1 \rightarrow j}^{o+1}$	χ_{j-1}	$e^{-\chi_{j-1}}$	$J_0(i\chi_{j-1})$	$-iJ_1(i\chi_{j-1})$
0 → 1	2.0605	.41399	.66107	1.04332	0.21140
1 → 2	4.0623	.80815	.44567	1.17009	0.43795
2 → 3	5.8405	1.16191	.31289	1.35710	.68469
3 → 4	7.3259	1.45741	.23284	1.60579	.94011
4 → 5	8.4565	1.68234	.18593	1.84306	1.17599
5 → 6	9.2004	1.83033	.16036	2.03043	1.35583
6 → 7	9.5514	1.90016	.14954	2.12622	1.44842
7 → 8	9.5349	1.89637	.15003	2.12331	1.44394
8 → 9	9.1985	1.82995	.16042	2.02993	1.35534
9 → 10	8.6026	1.71140	.19061	1.98777	1.20964
10 → 11	7.8191	1.55553	.21103	1.70280	1.03795
11 → 12	6.9189	1.37645	.25247	1.53261	.86461
12 → 13	5.9689	1.13745	.30499	1.38482	.70469
13 → 14	5.0246	.99959	.36802	1.26587	.56491
14 → 15	4.1310	.82182	.43963	1.17612	.44656
15 → 16	3.3190	.66028	.51670	1.11200	.34847
16 → 17	2.6084	.51092	.59516	1.06851	.26830
17 → 18	2.0051	.39839	.67106	1.04013	.20341
18 → 19	1.5082	.30004	.74079	1.02266	.15172
19 → 20	1.1110	.22102	.80170	1.01122	.11075
21 → 22	0.60567	.12049	.88647	1.00363	.06035
23 → 24	0.28645	.057384	.94423	1.00082	.02369
25 → 26	0.12692	.025249	.97506	1.00015	.01262
27 → 28	-.051642	.010274	.90978	1.0	.00514
29 → 30	.019455	.0038704	.99611	1.0	.00194
39 → 40	0.00000	0	1.0	1.0	0

TABLE XVI(b) (CONTINUED)

Transition $j - 1 \rightarrow j$	$J_0(i\chi_{j-1})$	$F(\chi_{j-1})$	$\frac{J_F(300)}{\nu^2}$	I_{j-1}
	$-i J_1(i\chi_{j-1})$			
0 → 1	1.25472	.17257	12.7551	12.7551
1 → 2	1.60804	.29113	12.5962	3.66713
2 → 3	2.05179	.37496	12.4402	4.66458
3 → 4	2.54590	.43427	12.2869	5.33533
4 → 5	3.01905	.47470	12.1363	5.76110
5 → 6	3.38626	.49960	11.9918	5.99110
6 → 7	3.57654	.51086	11.8476	6.05246
7 → 8	3.56725	.51031	11.7049	5.97313
8 → 9	3.38527	.49554	11.5675	5.73216
9 → 10	3.09741	.43126	11.4311	5.50133
10 → 11	2.74075	.45226	11.2958	5.10886
11 → 12	2.39742	.41879	11.1655	4.67600
12 → 13	2.03951	.38039	11.0363	4.19810
13 → 14	1.83078	.33854	10.9117	10.9117
14 → 15	1.62268	.29470	10.7881	3.17925
15 → 16	1.46047	.25047	10.6655	2.67139
16 → 17	1.33681	.20753	10.5477	2.18896
17 → 18	1.24359	.16733	10.4308	1.74539
18 → 19	1.17438	.13121	10.3144	1.35335
19 → 20	1.12197	.09993	10.2029	1.01958
21 → 22	1.06398	.05712	9.9856	.57038
23 → 24	1.02951	.02004	9.7793	.27421
25 → 26	1.01277	.01253	9.5926	.12020
27 → 28	1.00514	.005137	9.4149	.043364
29 → 30	1.00194	.001940	9.2425	.017930
29 → 40	1.0	*	8.4669	0

$$\sum I_{j-1} = 63.259$$

$$\mathcal{E}_2 = \frac{\sum I_{j-1}}{R_{0 \rightarrow \infty}} = \frac{63.259}{4.6166 \times 10^5} = 1.36349 \times 10^{-4}$$

TABLE XII (a)

WORK SHEET FOR THE CALCULATION OF R_A/μ^2 FOR THE FUNDAMENTAL VIBRATION-ROTATION RADIATION OF CO AT 300°K
 $(J \rightarrow J - 1)$

Transition $J \rightarrow J - 1$	Line Center $\mu(\text{cm}^{-1})$	$10^3 \lambda(\text{cm})$	λT	$R_A/R_{A,\text{max}}$	$10^7 R_A$	$10^{-6} \mu^2$	R_A/μ^2
1 → 0	2136.4	46764	• 14029	• 190127	5.93666	13.0920	
2 → 1	2134.6	468247	• 14054	• 191961	6.04440	4.55652	13.2659
3 → 2	2130.6	46935	• 14081	• 193940	6.10672	4.59446	13.4525
4 → 3	2126.6	47023	• 14107	• 195849	6.16683	4.62443	13.6361
5 → 4	2122.6	47112	• 14134	• 19783	6.22920	4.65443	13.8260
6 → 5	2118.6	47201	• 14160	• 19974	6.28935	4.68447	14.0122
7 → 6	2114.5	47293	• 14185	• 201791	6.35393	4.71111	14.2110
8 → 7	2110.4	47384	• 14215	• 203787	6.41578	4.75379	14.4075
9 → 8	2106.3	47483	• 14249	• 205966	6.49539	4.82650	14.6183
10 → 9	2102.1	475715	• 142715	• 207917	6.54632	4.81882	14.8158
11 → 10	2097.9	47667	• 143001	• 210015	6.61283	4.90118	15.0252
12 → 11	2093.6	47765	• 143295	• 21272	6.69306	4.98316	15.2813
13 → 12	2089.3	47863	• 143509	• 214329	6.74372	4.96117	15.4604
14 → 13	2085.0	47962	• 143836	• 216508	6.81733	4.94723	15.6820
15 → 14	2080.7	48061	• 144133	• 218636	6.88591	4.92931	15.9053
16 → 15	2076.3	48163	• 144430	• 220931	6.95660	4.911022	16.1968
17 → 16	2071.9	48265	• 144716	• 223176	7.02729	4.29277	16.3701
18 → 17	2067.4	48370	• 145110	• 225551	7.10207	4.27444	16.6164
19 → 18	2063.0	484731	• 145419	• 227971	7.17536	4.25597	16.8664
20 → 19	2058.4	48581	• 145743	• 230508	7.25316	4.23701	17.1304
22 → 21	2049.3	48797	• 146391	• 235582	7.41793	4.19663	17.6633
24 → 23	2040.1	49017	• 147051	• 240749	7.58063	4.16200	18.2139
26 → 25	2030.6	49247	• 147741	• 246152	7.75075	4.12324	18.7973
28 → 27	2021.1	49476	• 148324	• 251578	7.92161	4.04485	19.3927
30 → 29	2011.5	4974	• 149142	• 257122	8.09617	4.04613	20.0097
40 → 39	1961.4	509364	• 152952	• 288129	9.07251	3.84701	23.5533

TABLE XVII(b)

WORK SHEET FOR THE CALCULATION OF R_2/μ^2 FOR THE FUNDAMENTAL VIBRATION-ROTATION BAND OF CO AT 300°K
 $(J \rightarrow J + 1)$

Transition $J \rightarrow J + 1$	LINE CENTER $\mu(\text{cm}^{-1})$	$10^3 \lambda(\text{cm})$	λT	$R_2/R_{1,\text{max}}$	$10^{-7} R_2$	$10^{-6} \mu^2$	R_2/μ^2
0 → 1	2146.1	465962	1307836	13657	5.871455	4.605745	12.7551
1 → 2	2149.9	465138	1395444	18490	5.82207	4.62207	12.5962
2 → 3	2153.7	464317	139295	13324	5.76930	4.63642	12.4402
3 → 4	2157.4	463521	1390563	18162	5.71379	4.65437	12.2869
4 → 5	2161.1	462727	1388118	18001	5.66810	4.67035	12.1363
5 → 6	2164.7	461958	1385874	17846	5.61929	4.68593	11.9913
6 → 7	2168.3	461191	1383573	17690	5.57017	4.70152	11.8476
7 → 8	2172.9	460426	1381278	175351	5.52139	4.71715	11.7049
8 → 9	2175.4	459636	1379058	173851	5.47416	4.73237	11.5675
9 → 10	2178.9	459447	1376241	172354	5.42703	4.74760	11.4311
10 → 11	2182.4	458211	1374633	170862	5.38005	4.76237	11.2953
11 → 12	2185.8	457493	1372494	169417	5.32455	4.77772	11.1655
12 → 13	2189.2	456788	1370364	167978	5.28924	4.79260	11.0363
13 → 14	2192.5	456100	1368300	166583	5.24531	4.80706	10.9117
14 → 15	2195.8	455415	136624	165192	5.20151	4.82154	10.7331
15 → 16	2199.1	454731	136419	163807	5.15790	4.83604	10.6655
16 → 17	2202.3	454071	136221	162469	5.11577	4.85013	10.5477
17 → 18	2205.5	453412	1360236	161135	5.07377	4.86423	10.4306
18 → 19	2208.7	452755	135826	159310	5.03173	4.87336	10.3144
19 → 20	2211.3	452120	135636	158517	4.99133	4.89206	10.2029
21 → 22	2217.9	450377	135263	155997	4.91193	4.91903	9.9856
23 → 24	2223.9	449661	1348933	153599	4.83647	4.94573	9.7793
25 → 26	2229.7	448291	134547	151456	4.76900	4.97156	9.5926
27 → 28	2235.3	447367	134210	149359	4.70423	4.99657	9.4149
28 → 29	2240.5	446269	133530	147336	4.64034	5.02118	9.2425
30 → 31	2265.8	441345	132403	136373	4.35704	5.13305	8.4369

The results of more extensive emissivity calculations at 300°K and atmospheric pressure as a function of optical density are listed in Table XVIII.

TABLE XVIII

EMISSIVITIES AT 300°K AND ATMOSPHERIC PRESSURE FOR
NON-OVERLAPPING ROTATIONAL LINES ($\alpha = 0.06 \text{ cm}^{-1}$)

pL	Calculated Emissivity	Observed Emissivity ⁽⁹⁾
0.1 cm-atm	4.1266×10^{-4}	3.94×10^{-4}
0.5 " "	1.0805×10^{-3}	1.04×10^{-3}
2.0 " "	2.2124×10^{-3}	2.21×10^{-3}
6.0 " "	3.9048×10^{-3}	3.35×10^{-3}
30.0 " "	8.8403×10^{-3}	5.85×10^{-3}
70.0 " "	1.3547×10^{-2}	7.94×10^{-3}

Reference to Table XVIII indicates excellent agreement between calculated and observed emissivities for optical densities up to 2 cm-atm. At larger optical densities the calculated emissivities exceed the measured values. This result is in agreement with the conclusions reached in Section V.B from a study of overlapping between two adjacent rotational lines. This study suggested that overlapping cannot be ignored at pressures exceeding about 2 cm-atm. Thus the observed discrepancies between calculated and observed emissivities are the result of the fact that the mathematical techniques used for the calculation of emissivity break down at large optical densities. The data listed in Table XVII provide the first quantitative confirmation of the fact that empirically observed emissivities agree with emissivities calculated

from spectroscopic data at low optical densities. These results supplement the results of previous calculations^(5,6,7) which showed that the calculated temperature dependence of emissivity, as well as numerical values at large optical densities, agree with observed data.

C. Effect of Rotational Half-Width on Emissivity

Since the rotational half-width is probably the least reliably known physical constant entering into the problem of quantitative emissivity calculations, it is of obvious importance to determine the dependence of emissivity on the assumed rotational half-width for the condition of no overlapping between rotational lines. Representative results are summarized in Table XIX and plotted in Fig. 4. Reference to the data listed in Table XIX and shown in Fig. 4 indicates that the calculated emissivity is roughly proportional to the assumed value of the rotational half-width. Furthermore, agreement between calculated and observed emissivities is soon to be best for $\alpha = 0.06 \text{ cm}^{-1}$ at low optical densities. Since the best available estimate for α is 0.077 cm^{-1} for self-broadening⁽¹⁷⁾, the data of Fig. 4 suggest that broadening of the rotational lines of CO by air, which was used in the experiments of Hottel and Ullrich, must be about as effective as broadening by CO.

The results of the present calculations are of considerable practical importance in that it has not been realized in engineering calculations that the emissivity is a sensitive function of composition which determines the rotational half-width⁽¹⁷⁾. Thus we must conclude

TABLE XIX

TABULATED RESULTS OF CALCULATED AND OBSERVED INTENSITIES

$T = 300^{\circ}\text{K}$
 $\alpha = 0.06 \text{ cm}^{-1}$
Fundamental

pL (cm-atm)	pL (ft-atm)	$\sum I_j$ $j \rightarrow j - 1$	ϵ_1	$\sum I_{j-1}$ $j - 1 \rightarrow j$	ϵ_2	Σ $(\epsilon_1 + \epsilon_2)$
0.1	0.003278	92.159	1.9963 ⁻⁴	75.105	1.6269 ⁻⁴	3.4300 ⁻³
0.5	0.0164	237.439	5.1433 ⁻⁴	191.754	4.1537 ⁻⁴	9.2970 ⁻⁴
2.0	0.0656	494.314	1.0707 ⁻³	392.901	3.5110 ⁻³	1.9215 ⁻³
6.0	0.1965	896.957	1.9429 ⁻³	686.507	1.4571 ⁻³	3.4300 ⁻³

$T = 300^{\circ}\text{K}$
 $\alpha = 0.07 \text{ cm}^{-1}$
Fundamental

pL (cm-atm)	pL (ft-atm)	$\sum I_j$ $j \rightarrow j - 1$	ϵ_1	$\sum I_{j-1}$ $j - 1 \rightarrow j$	ϵ_2	Σ $(\epsilon_1 + \epsilon_2)$
0.1	0.003278	97.0395	2.101994 ⁻⁴	73.6516	1.703639 ⁻⁴	3.80568 ⁻⁴
0.5	0.0164	254.1265	5.50469 ⁻⁴	202.806	4.39303 ⁻⁴	9.39772 ⁻⁴
2.0	0.0656	534.296	1.157355 ⁻³	400.611	8.67772 ⁻⁴	2.02513 ⁻³
6.0	0.1965	940.700	2.03767 ⁻³	740.947	1.00496 ⁻³	3.66265 ⁻³
20.0	0.934	2240.674	4.63696 ⁻³	1666.900	3.61071 ⁻³	8.24737 ⁻³
70.0	2.2966	5277.341	7.099212 ⁻³	2547.922	5.51911 ⁻³	1.26132 ⁻²

TABLE XIX (CONTINUED)

TABULATED RESULTS OF CALCULATED AND OBSERVED EXTINCTION

 $T = 300^{\circ}\text{K}$
 $\alpha = 0.08 \text{ cm}^{-1}$
 Fundamental

pL (cm-atm)	$\frac{pL}{(\text{ft}-\text{atm})}$	$\sum I_{j-j'-1}$	ϵ_1	$\sum I_{j-j'-1}$ $j - 1 \rightarrow j$	ϵ_2	$\sum (\epsilon_1 + \epsilon_2)$	Ullrich
0.1	0.003275	107.249	2.32314 ⁻⁴	83.259	1.20349 ⁻⁴	4.12663 ⁻⁴	4.1×10^{-4}
0.5	0.0164	282.300	6.11497 ⁻⁴	216.501	4.68963 ⁻⁴	1.00046 ⁻³	1.05×10^{-3}
2.0	0.0656	571.496	1.23780 ⁻³	449.950	9.74549 ⁻⁴	2.21295 ⁻³	2.2×10^{-3}
6.0	0.1965	1010.640	2.18917 ⁻³	792.025	1.715623 ⁻³	3.90479 ⁻³	3.35×10^{-3}
30.0	0.984	2296.369	4.97422 ⁻³	1724.807	3.36611 ⁻³	8.40335 ⁻³	5.9×10^{-3}
70.0	2.2966	3530.923	7.64842 ⁻³	2723.093	5.39655 ⁻³	1.35497 ⁻²	
$T = 300^{\circ}\text{K}$ $\alpha = 0.063 \text{ cm}^{-1}$							
Overtone (1st)							
pL (cm-atm)	$\frac{pL}{(\text{ft}-\text{atm})}$	$\sum I_{j-j'-1}$	ϵ_1	$\sum I_{j-j'-1}$ $j - 1 \rightarrow j$	ϵ_2	$\sum (\epsilon_1 + \epsilon_2)$	
0.1	0.003278	0.357297	7.73957 ⁷	0.284072	6.19667 ⁷	1.39361 ⁻⁶	
0.5	0.0164	1.748115	3.78666 ⁻⁶	1.39784	3.0322 ⁻⁵	6.8135 ⁻⁶	
2.0	0.0656	6.468213	1.40109 ⁻⁵	5.13536	1.11230 ⁻⁵	2.51347 ⁻⁵	
6.0	0.1963	16.33507	3.52337 ⁻⁵	12.35345	2.7842 ⁻⁵	6.3225 ⁻⁵	
30.0	0.9842	48.11283	1.067215 ⁻⁴	36.30793	7.9734 ⁻⁵	1.63952 ⁻⁴	
70.0	2.2965	78.01510	1.6399 ⁻⁴	59.22354	1.23226 ⁻⁴	2.97236 ⁻⁴	

that not only is it not justified to extrapolate emissivities indiscriminately over temperature, pressure, or optical density intervals by using unsound simplified equations, but it is also essential to consider the problem with the proper regard for the concentration of infrared-inert gases.

D. Emission of Radiation from the First Overtone of CO at 300°K and Atmospheric Pressure

In the comparisons presented in Sections V.B and V.C between calculated and observed emissivities, contributions from the first overtone and upper harmonics have been ignored. The intensity of radiation emitted from these vibration-rotation bands should, of course, be included in the calculated values of the emissivity. However, it is a simple matter to show that for the conditions for which overlapping between rotational lines is negligibly small, the contributions to the emissivity from overtone transitions are also negligibly small.

Representative numerical values based on the use of Eq. (31) and of the integrated absorption values listed in Table X lead to the overtone emissivities listed in Table XIX as a function of optical density. It is evident from Table XIX that the first overtone contributions to the emissivity, for conditions for which a treatment based on non-overlapping rotational lines is valid, are, in fact, less than 2%.

VI. CONCLUSIONS AND RECOMMENDATIONS FOR FURTHER STUDY

The salient conclusions of the present analysis have already been described but are enumerated here for convenience. They are

- (1) Emissivities calculated by reliable methods from the best available spectroscopic data at low optical densities and room temperature agree quantitatively with experimental measurements.
- (2) The limits of validity of a treatment based on non-overlapping rotational lines are defined conservatively by a consideration of overlapping between two intense adjacent rotational lines. This conclusion can, no doubt, be made more quantitative and less restrictive by a more detailed study of the basic relations. However, time did not permit further consideration of partial overlapping between rotational lines.
- (3) The emissivity at low optical densities is, approximately, a linear function of rotational half-width. This result emphasizes the need for reliable half-width measurements as a function of composition, pressure, and temperature.

Important problems which require further study are the following:

- (1) Emissivity calculations for partial overlapping between rotational lines, in order to bridge the gap between the treatments based on the assumption of non-overlapping between rotational lines and complete overlapping between rotational lines^(5,6,7).
- (2) Emissivity calculations at elevated temperatures for non-overlapping rotational lines, in order to demonstrate that the temperature-dependence of emissivity is calculated correctly. The mathematical techniques for this calculation have all been worked out and

applied to a problem on temperature measurements. (3)

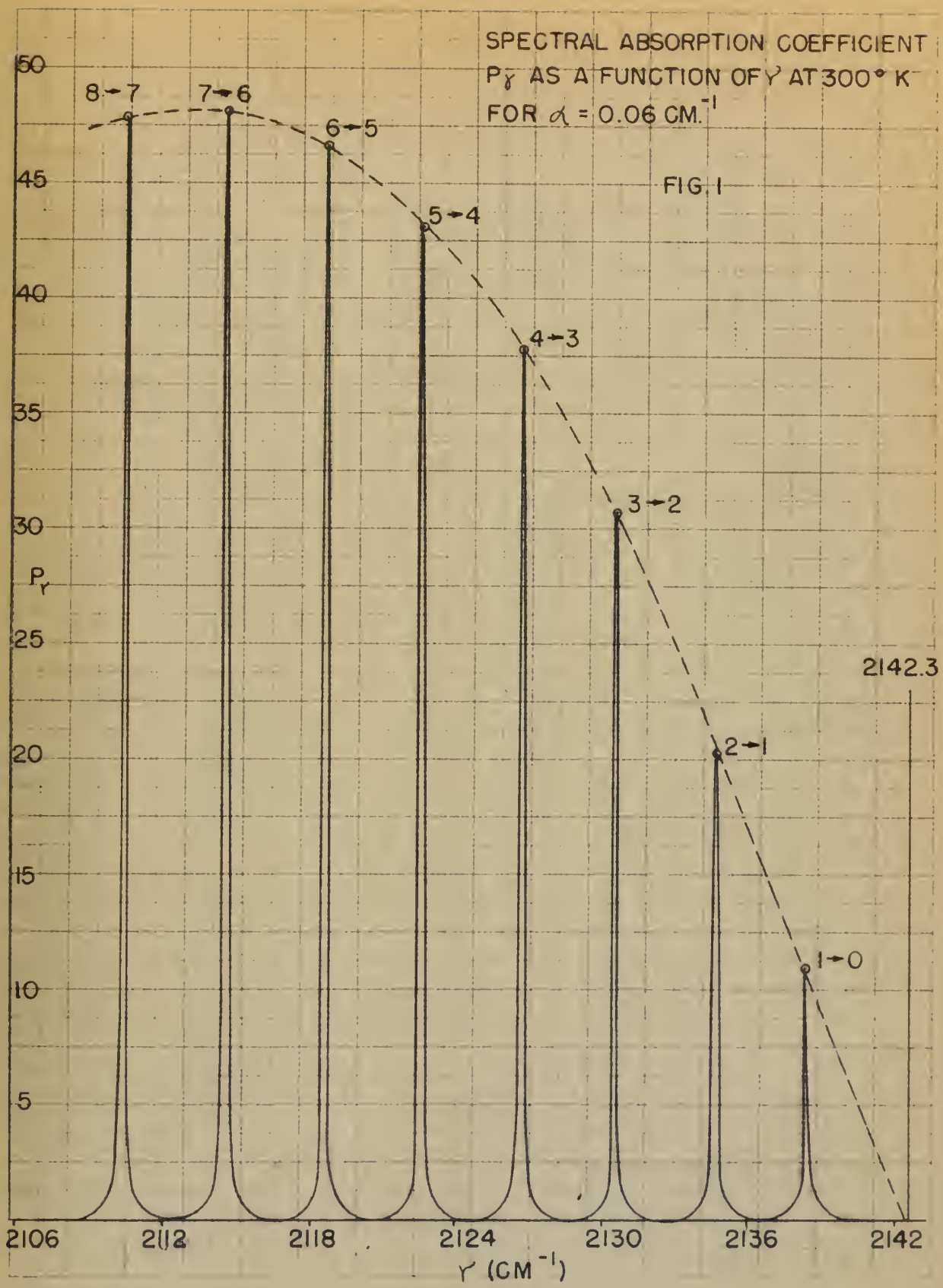
(3) It is apparent at the present time that a tabulation of gaseous emissivities, even for diatomic molecules, cannot be carried out completely without the use of automatic computing machines. For this reason, consideration should be given to standardization of techniques adaptable to machine calculations, particularly at elevated temperatures, where the entire problem of emissivity calculations is enormously complicated by overtone transitions.

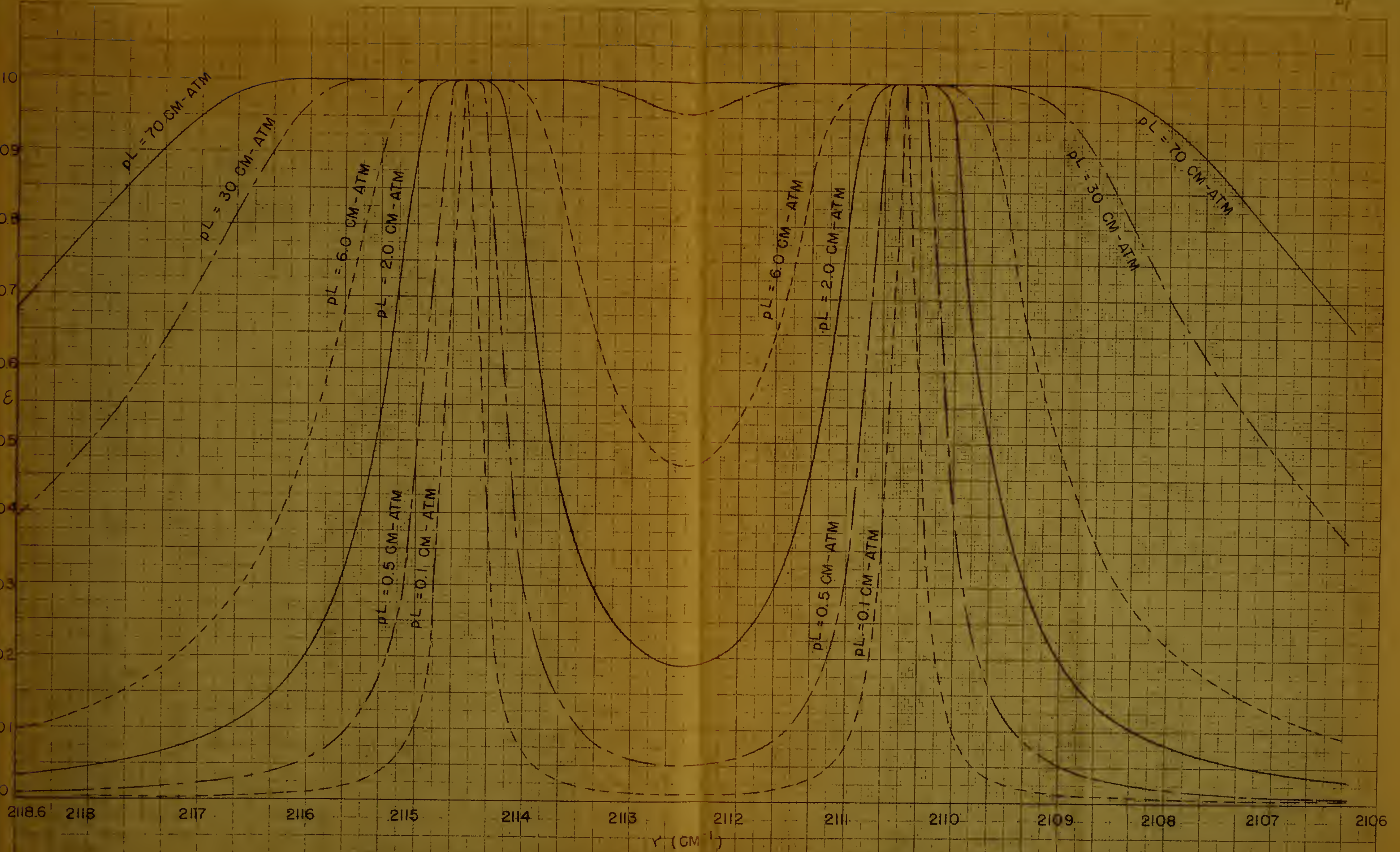
(4) The entire program of emissivity calculations of gases is based on accurate knowledge of experimental data on integrated absorption and rotational half-width. It is therefore obvious that the present program depends upon the accurate measurement of the required spectroscopic constants. Further extensive studies of this type are being carried out at the Jet Propulsion Laboratory.

REFERENCES

1. S. Chandrasekhar, Radiative Transfer, Clarendon Press, Oxford, (1950).
2. S. S. Penner, Am. J. Phys., 17 491, (1949).
3. W. M. Elsasser, Harvard Meteorological Studies No. 6, Blue Hill Observatory, Milton, Mass., (1942).
4. D. H. Dennison, Phys. Rev. 31 503, (1923).
5. S. S. Penner, J. Appl. Phys. 21 685, (1950).
6. S. S. Penner, J. Appl. Mech. 12, (1951).
7. L. E. Benitez and S. S. Penner, J. Appl. Phys. 21 907, (1950).
8. S. S. Penner, J. Chem. Phys. 19 272, (1951).
9. K. C. Hottel, Heat Transmission by Radiation from Non-Luminous Gases, TRAIS, A.I.C.E. 12 173, (1927).
W. Ullrich, Heat Transmission by Radiation from Non-Luminous Gases, Experimental Study of Carbon Monoxide, N.I.T., (1935).
10. J. E. Mayer and M. G. Mayer, Statistical Mechanics, John Wiley and Sons, N. Y., (1946).
11. H. Sponer, Molekülspektren, J. Springer, Berlin, (1935).
12. G. Herzberg, Atomic Spectra and Atomic Structure, Dover Publications, New York, (1944); Spectra of Diatomic Molecules, D. Van Nostrand Co., New York, (1950); Infrared and Raman Spectra of Polyatomic Molecules, D. Van Nostrand Co., New York, (1950).
13. H. Margenau and W. W. Watson, Rev. Mod. Phys. 8 22, (1936).
J. H. Van Vleck and V. F. Weisskopf, Rev. Mod. Phys. 17 227, (1945).
T. W. Anderson, Phys. Rev. 76 647, (1949).
Lindholm, E., Dissertation, Uppsala, (1942).
14. J. R. Oppenheimer, Proc. Camb. Phil. Soc. 23 327, (1936).
15. B. L. Crawford, Jr. and H. L. Dinsmore, J. Chem. Phys., 18 963, (1950).
16. K. Scholz, Zeits. f. Phys., 76 751, (1932).
17. Jet Propulsion Laboratory Report 9-2, September 1950,
Infrared Intensity and Line Width Measurements of Carbon Monoxide.
S. S. Penner-D. Weber.

18. Gray, Mathews, and MacRobert, Bessel Functions, MacMillan and Co., London, (1931).
19. Miscellaneous Physical Tables, Planck's Radiation Functions and Electronic Functions, Federal Works Agency, Work Projects Administration for the City of New York.
20. Jahnke, E. and F. Emde, Tables of Functions with Formulae and Curves, Dover Publications, (1943).





SPECTRAL EMISSIVITY AS A FUNCTION OF WAVE NUMBER FOR VARIOUS OPTICAL DENSITIES
FOR TWO ADJACENT INTENSE ROTATIONAL LINES ($U = 8 \rightarrow J = 7$ AND $J = 7 \rightarrow J = 6$)

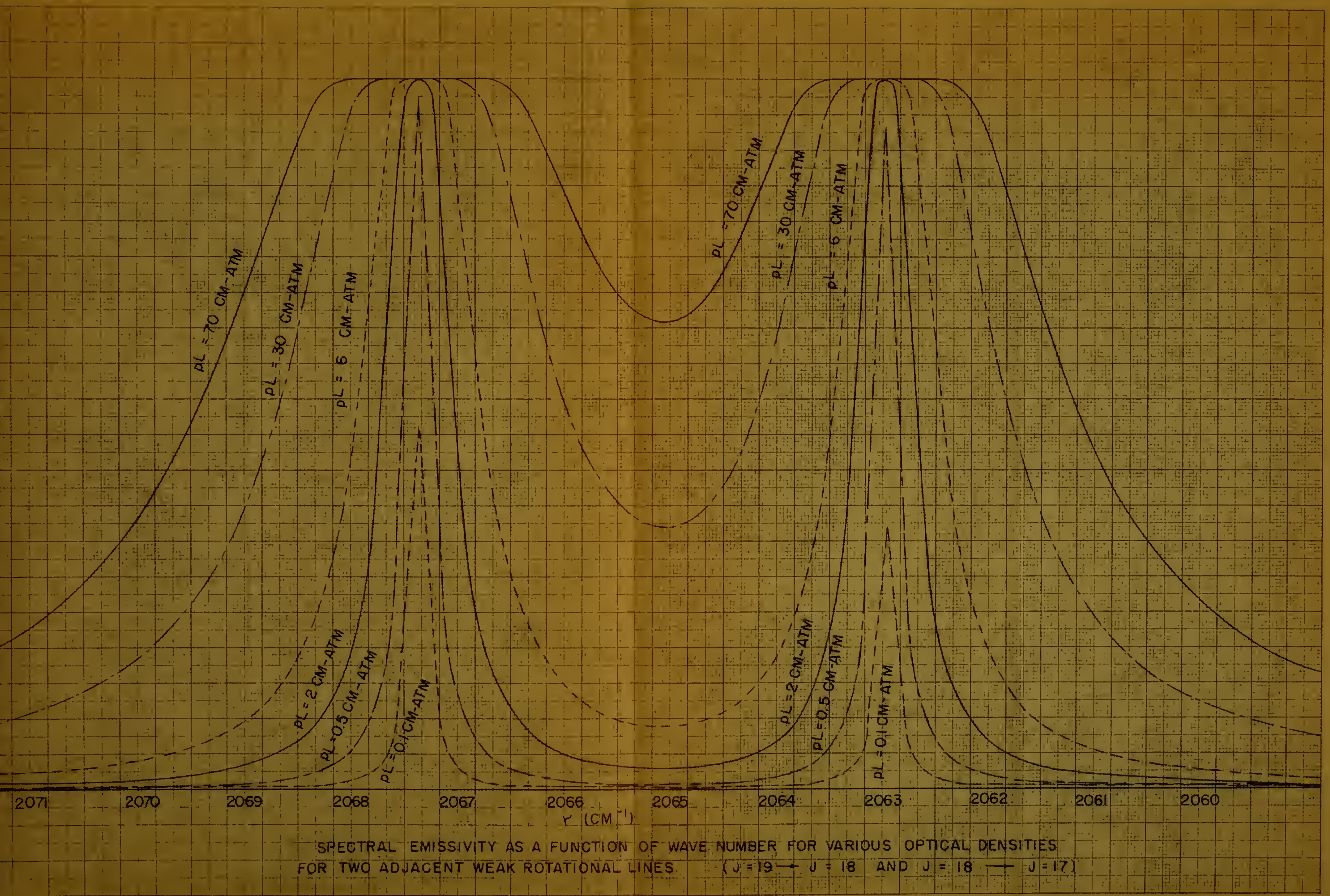
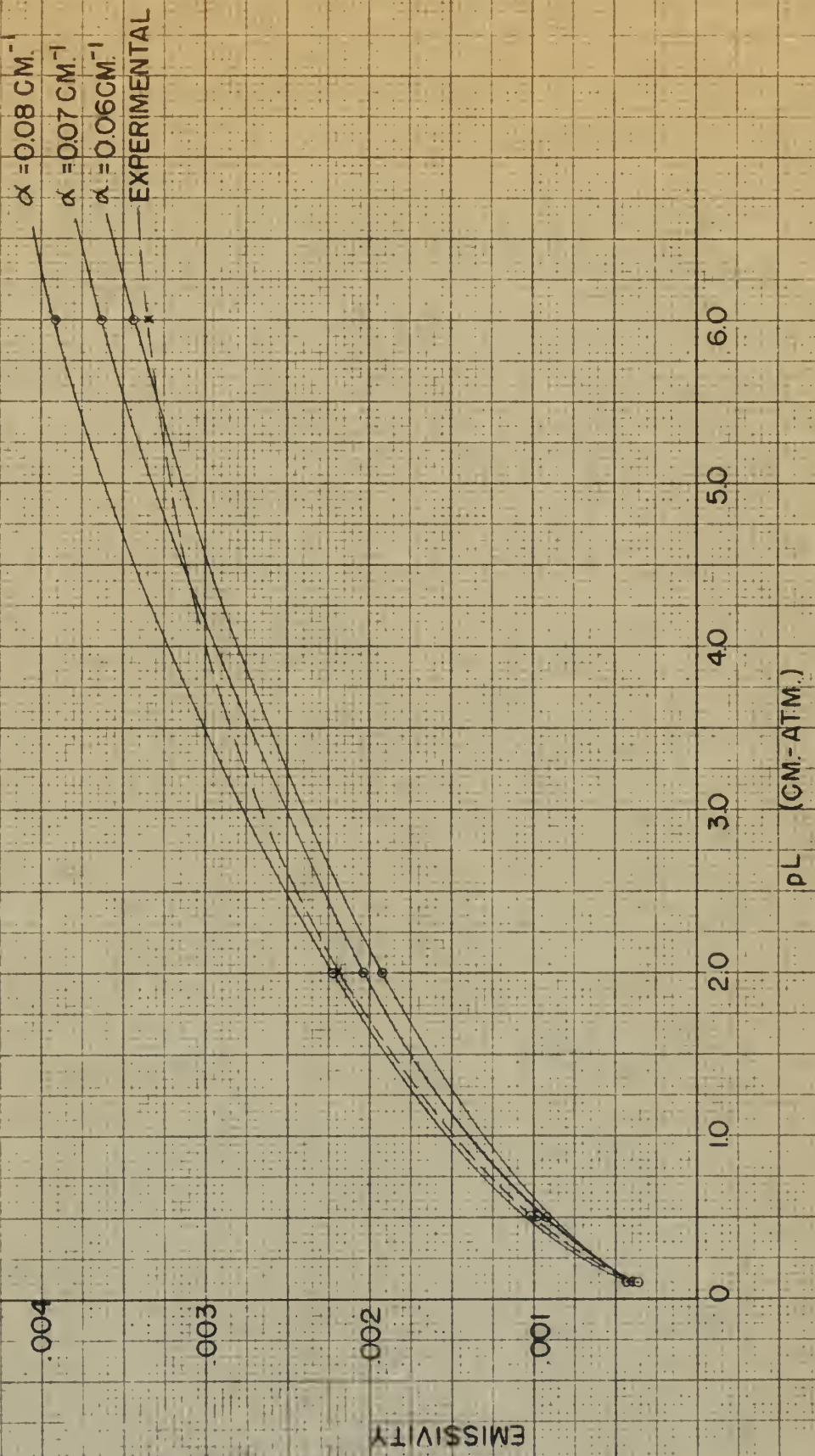


FIG. 3



VARIATION OF CALCULATED EMISSIVITY WITH SPECTRAL HALF-WIDTH

FIG. 4

Thesis 15647
086 Ostrander
Emissivity calculation
for carbon monoxide.

Thesis 15647
086 Ostrander
Emissivity calculation
for carbon monoxide.

thes086
Emissivity calculation for carbon monoxi



3 2768 001 97412 4
DUDLEY KNOX LIBRARY